

AMERICAN MUSEUM NOVITATES

Number 3833, 40 pp.

April 30, 2015

A new species of scaphitid ammonite from the lower Maastrichtian of the Western Interior of North America, with close affinities to *Hoploscaphites constrictus* Sowerby, 1817

NEIL H. LANDMAN,¹ W. JAMES KENNEDY,² AND NEAL L. LARSON³

ABSTRACT

We describe a new species of scaphitid ammonite from the Upper Cretaceous (lower Maastrichtian) of North America. *Hoploscaphites sargklofak*, n. sp., is endemic to the U.S. Western Interior, but closely resembles *H. constrictus* Sowerby, 1817, from the Maastrichtian of northern Europe.

INTRODUCTION

We describe a new species of *Hoploscaphites* (Ammonoidea: Ancyloceratina) from the Upper Cretaceous (lower Maastrichtian) of the Pierre Shale of Colorado, Wyoming, and South Dakota, the Lewis Shale of Wyoming, and the Bearpaw Shale of Montana. *Hoploscaphites sargklofak*, n. sp., is strongly dimorphic with a compressed whorl section and a circular to oval outline in lateral view. The adult is characterized by fine flexuous ribs, small, closely spaced ventrolateral tubercles, which become more closely spaced near the aperture, umbilicolateral tubercles or bullae on the shaft of the body chamber, and one or two rows of lateral tubercles on the adapical part of the phragmocone, and more rarely, on the hook. This spe-

¹ Division of Paleontology (Invertebrates), American Museum of Natural History.

² Oxford University Museum of Natural History, Oxford, United Kingdom.

³ Larson Paleontology Unlimited, Hill City, SD.

Stage	U.S. Western Interior Ammonite Zones	Age (Ma)	
Maastrichtian	lower	<i>Baculites clinolobatus</i>	69.59 ± 0.36
		<i>Baculites grandis</i>	70.00 ± 0.45
		<i>Baculites baculus</i>	
Campanian	upper	<i>Baculites eliasi</i>	71.98 ± 0.31
		<i>Baculites jenseni</i>	
		<i>Baculites reesidei</i>	72.94 ± 0.45 ¹
		<i>Baculites cuneatus</i>	
		<i>Baculites compressus</i>	73.52 ± 0.39 ²
		<i>Didymoceras cheyennense</i>	74.67 ± 0.15
		<i>Exiteloceras jenneyi</i>	75.08 ± 0.11 ²
		<i>Didymoceras stevensoni</i>	
		<i>Didymoceras nebrascense</i>	75.19 ± 0.28

¹ ⁴⁰Ar/³⁹Ar on sanidine as corrected by Baadsgaard (1993);
² low in zone; ³ Izett et al. (1998)

FIG. 1. Upper Cretaceous (Campanian and Maastrichtian) ammonite biostratigraphy of the U.S. Western Interior showing the Zone of *Baculites grandis* (Cobban et al., 2006). The absolute ages are derived from ⁴⁰Ar/³⁹Ar analysis of bentonites containing sanidines.

zones. This zonation has been integrated with radiometric dates owing to the presence of interbedded bentonites (fig. 1). *Hoploscaphites sargklofak*, n. sp., occurs in the *Baculites grandis* Zone, which occupies the middle part of the lower Maastrichtian, approximately 70 million years ago (fig. 2).

The Western Interior Seaway extended from the western Canadian Arctic to the proto-Gulf of Mexico (Gill and Cobban, 1966; Kauffman, 1967; Kauffman and Caldwell, 1993). During the early Maastrichtian, the shoreline cut across the eastern half of Montana and formed a broad delta (the Sheridan Delta) at the southeastern corner of Montana and the northeastern corner of Wyoming (Cobban et al., 1994). The shoreline continued as a series of embayments across Wyoming as far as the northwest corner of Colorado and then cut northwest-southeast across the middle of the state (fig. 3). *Hoploscaphites sargklofak*, n. sp., was especially abundant in the northeast corner of Wyoming in the embayment just south of the Sheridan Delta, although this may simply reflect

cies closely resembles *H. constrictus* Sowerby, 1817, from the Maastrichtian of northern Europe, but differs from it in terms of its shape and the details of its ornamentation: (1) in *H. sargklofak*, n. sp., the number of ventrolateral tubercles on the exposed phragmocone is higher than in *H. constrictus*; (2) in *H. sargklofak*, n. sp., the venter of the shaft is flatter and the distance between ventrolateral tubercles on either side of the venter at midshaft is greater than that in *H. constrictus*; (3) in *H. sargklofak*, n. sp., one or two rows of lateral tubercles occasionally occur on the adapical part of the phragmocone and, more rarely, on the hook, whereas no such tubercles are present in either area in *H. constrictus*; and (4) in *H. sargklofak*, n. sp., the umbilicus is larger than that in *H. constrictus*.

GEOLOGIC SETTING

On the basis of previous studies, the Maastrichtian of the U.S. Western Interior has been subdivided into six zones (Gill and Cobban, 1966; Landman and Waage, 1993; Larson et al., 1997; Cobban et al., 2006). They are, from oldest to youngest, the *Baculites baculus*, *Baculites grandis*, *Baculites clinolobatus*, *Hoploscaphites birkelundae*, *Hoploscaphites nicolletii*, and *Hoploscaphites nebrascensis*

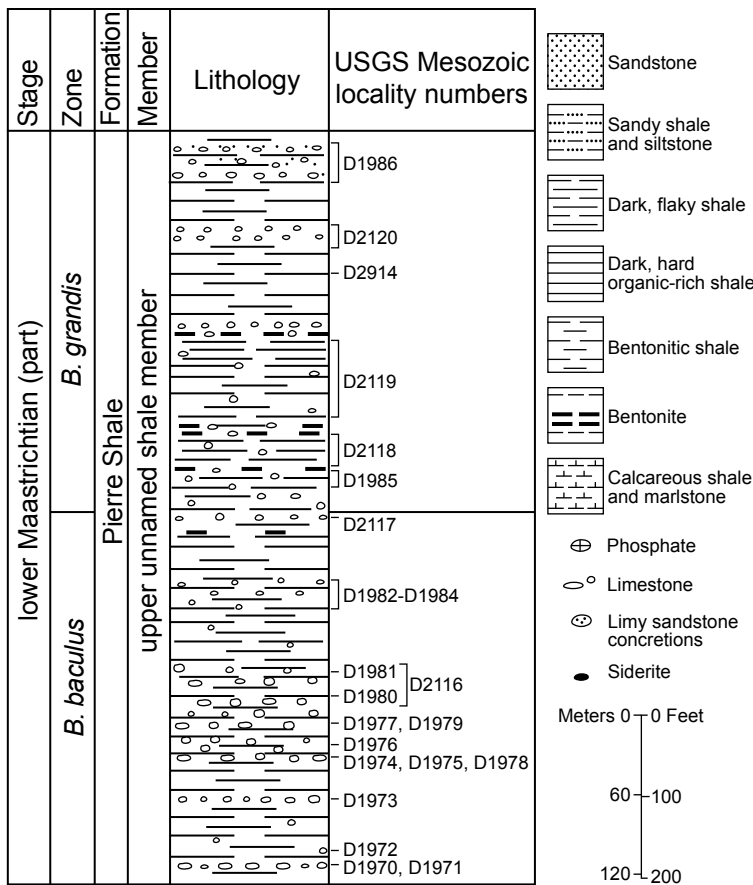


FIG. 2. Stratigraphic section of the upper unnamed member of the Pierre Shale at Red Bird, Niobrara County, Wyoming, showing the position of several USGS Mesozoic localities (after Gill and Cobban, 1966).

the distribution of outcrops. Localities mentioned in the text are illustrated in figure 3 and described in the appendix.

Williams and Stelck (1975: text-fig. 8) suggested that the seaway during this time also extended to the Atlantic Ocean via Hudson Bay and around the southern tip of Greenland. According to them, it also extended to the Arctic Ocean via the Mackenzie Valley, to west Greenland via Baffin Bay, and to the North Atlantic around the north end of Greenland. Indeed, the strong resemblance between *Hoploscaphites sargklofak*, n. sp., and *H. constrictus* from northern Europe suggests the existence of a northern connection between the Western Interior Seaway and the Atlantic Ocean. However, no early Maastrichtian ammonites have ever been reported from Canada (Riccardi, 1983) or Greenland (Birkelund, 1965), although this may be due to post-Cretaceous erosion.

TERMS, METHODS, AND REPOSITORIES

Landman et al. (2010) reviewed the terms used to describe scaphites. The adult shell consists of two parts, a closely coiled phragmocone and a slightly to strongly uncoiled body



FIG. 3. Map of the lower Maastrichtian *Baculites grandis* Zone showing the shoreline along the western margin of the Western Interior Seaway (based on Gill and Cobban, 1966). The numbered dots indicate AMNH, USGS, and YPM localities cited in the text, as listed in the appendix.

chamber (fig. 4). The part of the phragmocone that is exposed in the adult shell (as compared to the part that is concealed inside) is called the adult phragmocone. The most adapical point of the adult phragmocone is called the point of exposure. The body chamber consists of the shaft, beginning near the last septum, and a hook terminating at the aperture. The point at which the hook curves backward is called the point of recurvature.

Scaphites occur as dimorphs, which are referred to as macroconchs (M) and microconchs (m). They are interpreted as sexual in nature, the macroconch being the female, and the microconch being the male, after the traditional view as described by Cobban (1969), Landman and Waage (1993), and Davis et al. (1996).

Measurements of the adult shell are the same as those described and illustrated in Landman et al. (2013: 9, fig. 3). All measurements were made using electronic calipers on actual specimens, rather than on photos, with the exception of the apertural angle.

LMAX, maximum length from the venter of the phragmocone to the venter of the hook
UD, umbilical diameter through the center of the umbilicus parallel to the line of maximum length

W_p, whorl width of the phragmocone along the line of maximum length

H_p, whorl height of the phragmocone along the line of maximum length

W_s, whorl width of the body chamber at midshaft

H_s, whorl height of the body chamber at midshaft

W_H, whorl width of the hook at the point of recurvature

H_H, whorl height of the hook at the point of recurvature

V_s, width of the venter at midshaft as measured between the ventrolateral margins on opposite sides of the venter

AA, in macroconchs, the angle of intersection (in degrees) between two lines (a line drawn along the umbilical shoulder and another line drawn along the apertural margin), extending from approximately the point of recurvature to the aperture.

Several ratios were calculated to describe the shape of the adult shell and facilitate comparisons among specimens:

W_p/H_p, the ratio of whorl width to whorl height of the phragmocone along the line of maximum length

W_s/H_s, the ratio of whorl width to whorl height of the body chamber at midshaft

W_H/H_H, the ratio of whorl width to whorl height of the hook at the point of recurvature

V_s/H_s, the ratio of ventral width to whorl height at midshaft

LMAX/H_p, the ratio of maximum length to whorl height of the phragmocone along the line of maximum length

LMAX/H_s, in macroconchs, the ratio of maximum length to whorl height of the body chamber at midshaft

A number of terms are used to describe ornamentation:

primary ribs, ribs that originate near the umbilicus

secondary ribs, ribs that originate on the flanks or venter, either by branching or intercalation

rib density, number of ribs/cm on the venter as measured on the phragmocone along the line of maximum length, the midshaft, and the hook

tubercles, small conical swellings

bullae, swellings elongated in a radial direction

umbilicolateral bullae, bullae that occur near the umbilicolateral margin

ventrolateral tubercles, tubercles that occur near the ventrolateral margin

number of bullae/tubercles, number of bullae/tubercles as measured on the phragmocone, body chamber, or the entire adult shell

distance between bullae/tubercles, distance between bullae/tubercles following the curvature of the shell on the umbilicolateral margin for umbilicolateral bullae, and on the ventrolateral margin for ventrolateral tubercles

height of tubercle, tubercle height measured from the base to the tip

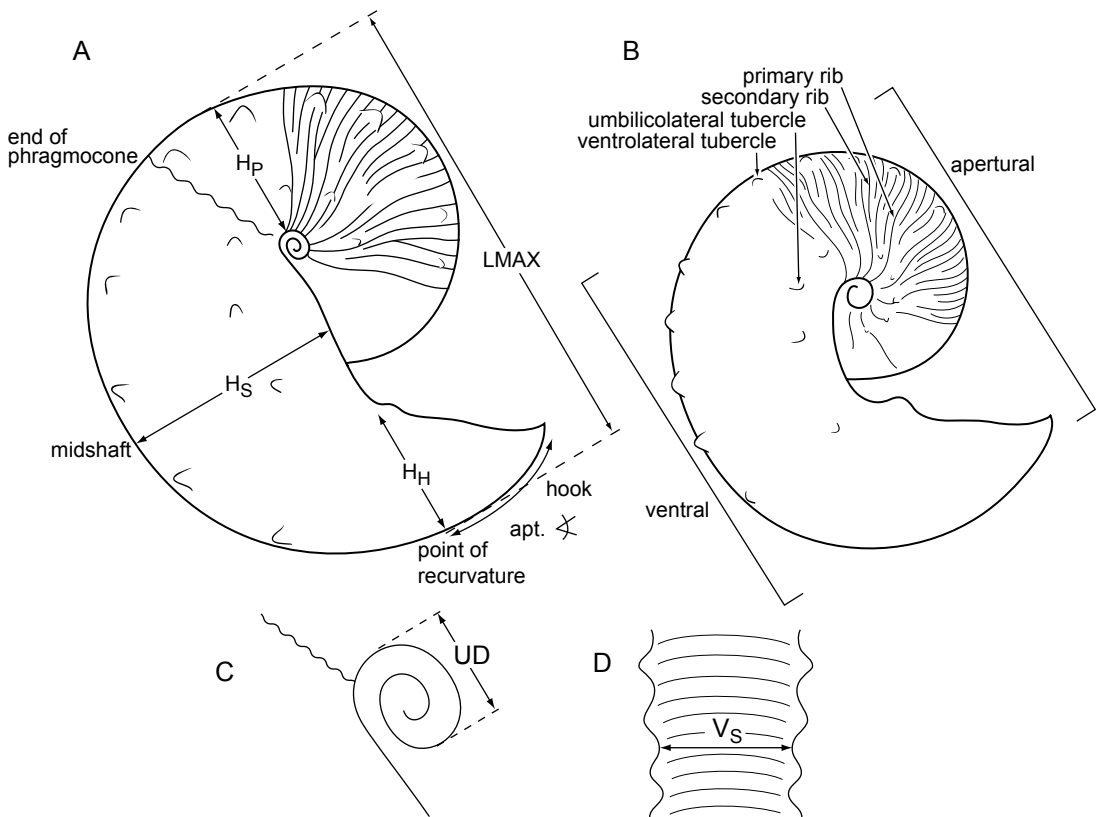


FIG. 4. Scaphite terminology (after Landman et al., 2013: 9, fig. 3). **A.** Macroconch, right lateral view. The shell is oriented in the probable floating position when the body was withdrawn into the body chamber. The umbilical seam of the shaft in macroconchs is straight with a slight umbilical bulge. Abbreviations: H_p = whorl height along the long axis; H_s = whorl height at midshaft; H_h = whorl height at the point of recurvature; LMAX = maximum length along the long axis; apt. \angle = apertural angle. **B.** Microconch, right lateral view. In *Hoploscaphites sargklofak*, n. sp., the microconch is 69% of the size of the macroconch or, inversely, the macroconch is 145% of the size of the microconch. The umbilical seam of the shaft in microconchs is curved and follows the curvature of the venter. Specimens are photographed from lateral, ventral, and apertural views, as shown. **C.** Close-up of the umbilicus of the macroconch showing the umbilical diameter measured parallel to the long axis (UD). **D.** View of the venter of the body chamber at midshaft, with the adoral direction toward the top, showing the width of the venter (V_s), as measured between the ventrolateral margins.

Photographs of adult shells are natural size. Small tick marks on the photos mark the base of the body chamber, where visible. The base of the body chamber is defined as the position of the median saddle in the ventral lobe.

The repository of specimens described in the text is indicated by a prefix: Division of Paleontology (Invertebrates), American Museum of Natural History (AMNH), New York; Black Hills Museum of Natural History (BHI), Hill City, South Dakota; British Museum (Natural History) (BMNH), London; Collections of the Sorbonne (SP), now in the Université Pierre et Marie Curie, Paris; Muséum National d'Histoire Naturelle (MNHP), Paris; Yale Peabody Museum (YPM), New Haven, Connecticut; and U.S. National Museum (USNM), Washington, D.C. The localities of the specimens are shown in figure 3 and are listed in the appendix.

SYSTEMATIC PALEONTOLOGY

Class Cephalopoda Cuvier, 1797

Order Ammonoidea Zittel, 1884

Suborder Ancyloceratina Wiedmann, 1966

Superfamily Scaphitoidea Gill, 1871

Family Scaphitidae Gill, 1871

Subfamily Scaphitinae Gill, 1871

Genus *Hoploscaphites* Nowak, 1911

[= *Mesoscaphites* Atabekian, 1979: 523 (nomen nudum) fide Kennedy, 1986; Wright, 1996; *Jeletzkytes* Riccardi, 1983: 14]

TYPE SPECIES: *Ammonites constrictus* J. Sowerby (1817: 189, pl. A, fig. 1), by original designation.

DIAGNOSIS: "Small to large scaphites, strongly dimorphic, with broad variation in degree of whorl compression ranging from slender to robust, with involute phragmocone, short to long shaft, and weakly recurved hook; apertural angle ranging from approximately 35° to 85°; aperture constricted with dorsal projection; ribs straight to flexuous, increasing by branching and intercalation, with weak to strong adoral projection on venter; adult shell with or without umbilicolateral, flank, and ventrolateral tubercles; suture fairly indented, with symmetrically to slightly asymmetrically bifid first lateral lobe" (Landman et al., 2010: 93).

DISCUSSION: The genus *Jeletzkytes* was synonymized with *Hoploscaphites* by Wright (1996) and Landman et al. (2010). These authors argued that the two genera share the same shell shape, pattern of ornamentation, and suture, and differ only in the degree of whorl compression and, as a consequence, the flexuosity of the ribs and size of the tubercles. Recently, Larson (in press) has suggested that *Jeletzkytes* should be treated as a subgenus of *Hoploscaphites* to distinguish the more robust end members of *Hoploscaphites*. This hypothesis requires testing using a phylogenetic analysis of all of the species in the genus.

Hoploscaphites sargklofak, n. sp.

Figures 5–21

DIAGNOSIS: Macroconchs oval to nearly circular in lateral view; cross section of shaft subquadrate with subparallel and nearly flat flanks converging toward the ventrolateral shoulder; large to moderately large umbilicus commonly with umbilical bulge; closely spaced ventrolateral tubercles with maximum spacing on the adoral part of shaft; umbilicolateral tubercles or bullae on body chamber; one or two rows of lateral tubercles occasionally on the adapical part of the phragmocone and, more rarely, scattered near the aperture; apertural angle averaging approximately 40°. Microconchs oval to nearly circular in lateral view; cross section of shaft subquadrate with broadly rounded to flattened flanks converging toward the ventrolateral shoulder; large umbilicus exposing earlier whorls; moderately widely to closely spaced ventrolateral tubercles becoming more widely spaced on adoral part of shaft; relatively prominent umbilicolateral tubercles on the body chamber; one or two rows of lateral tubercles occasionally present on the phragmocone.



FIG. 5. Assemblage of *Hoploscaphites sargklofak*, n. sp., macroconchs and microconchs (AMNH 63552–63555, 90566), associated with a specimen of *Baculites grandis* (AMNH 64669, bottom) in a single concretion from AMNH locality 3435 in the *B. grandis* Zone of the upper part of the Pierre Shale, Meade County, South Dakota. Note that the macroconch on the right has a big piece of shell missing from the adapical part of the body chamber leaving a jagged hole (arrow), indicating a lethal injury. Specimens $\times 1$.

ETYMOLOGY: This species is named in honor of Kathleen B. Sarg and Susan M. Klofak at the AMNH, who, over the span of more than 20 years, tirelessly helped collect, prepare, measure, and number all of the specimens used in this and many other studies of scaphites from the U.S. Western Interior and Gulf and Atlantic Coastal Plains. The species name is formed as a noun in apposition. Suggested pronunciation with soft g (as in *gel*).

TYPES: The types are from the *Baculites grandis* Zone of the Pierre Shale in Wyoming and the Bearpaw Shale in Montana. The holotype USNM 605788 (fig. 11A–D) is a macroconch from USGS locality 24312, McCone County, Montana. It is a steinkern 53.8 mm in diameter with a moderately large umbilicus and umbilical bulge. The macroconch paratypes are USNM 605796 (fig. 11I–L) from USGS Mesozoic locality D2118, Niobrara County, Wyoming, AMNH 74365 (fig. 14G–I) and 74366 (fig. 15D–F) from AMNH localities 3728 and 3727, respectively, Niobrara County, Wyoming, and USNM 605792 (fig. 14A–C) from USGS Mesozoic locality D11783, Weston County, Wyoming. The microconch paratypes are AMNH 74316 (fig. 18U–X) and 74319 (fig. 19O–Q) from AMNH localities 3728a and 3728, respectively, Niobrara County, Wyoming, and USNM 605812 (fig. 19R–T) from USGS locality 23625, Richland County, Montana.

MATERIAL: The collection consists of approximately 100 specimens of which 70 comprise the measured set. A total of nine specimens have been recovered from a single concretion from AMNH locality 3435 in the *Baculites grandis* Zone of the Pierre Shale, Meade County, South Dakota (fig. 5). All of the specimens in our collection are derived from the *B. grandis* Zone of the Pierre Shale of South Dakota, Wyoming, and Colorado, the Lewis Shale of Wyoming, and the Bearpaw Shale of Montana.

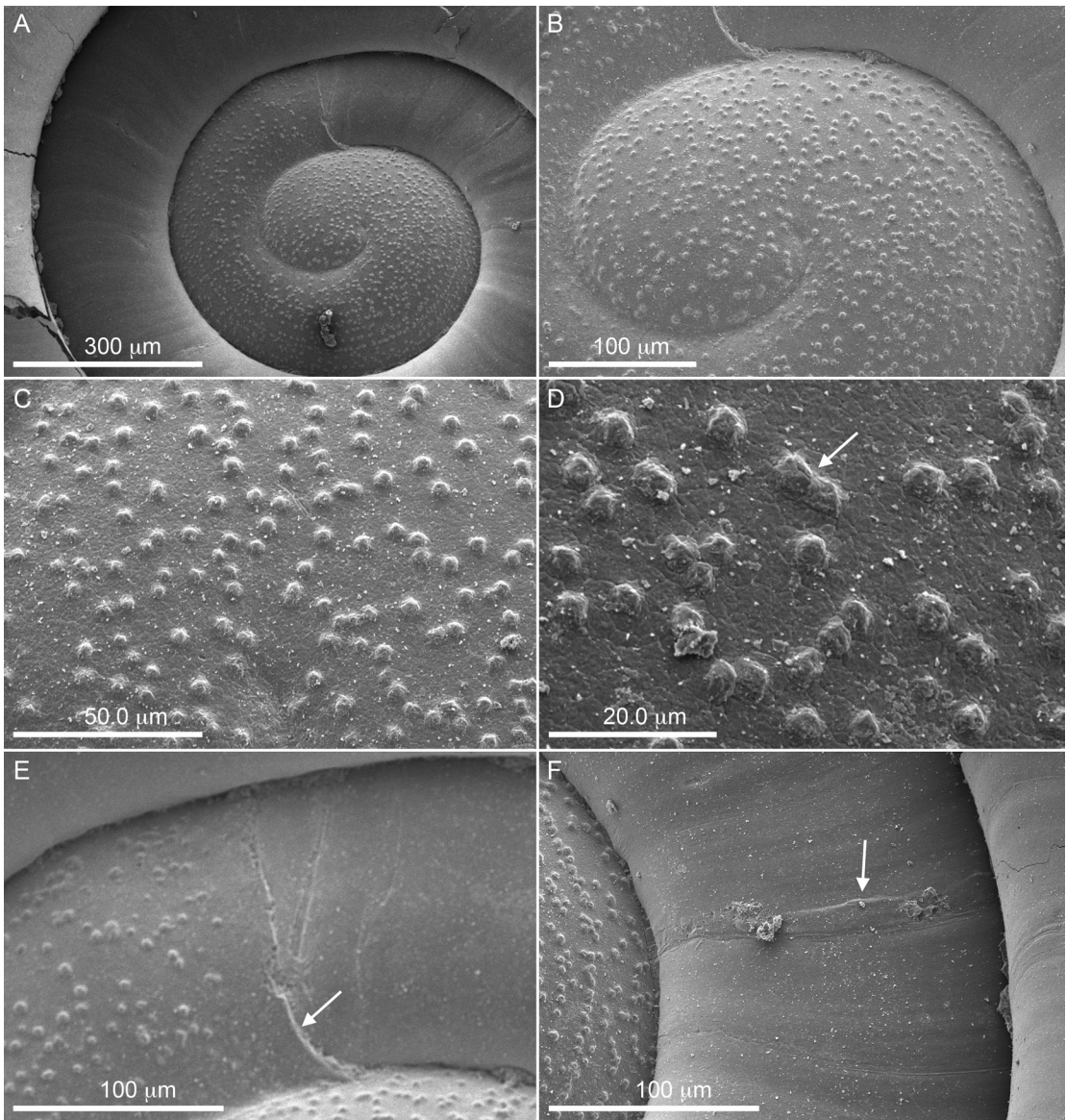


FIG. 6. Early whorls of *Hoploscaphites sargklofak*, n. sp. A–F. AMNH 63589, AMNH loc. 3278, Weston County, Wyoming. **A.** Overview of the tuberculate microornamentation on the ammonitella. **B.** Several of the tubercles on the initial chamber are arranged in rows near the ventrolateral margin. **C.** Close-up of the microornamentation on the initial chamber showing the uneven distribution of tubercles. **D.** Close-up of the tubercles on the initial chamber showing that some of them are fused together (arrow). **E.** Overview of the primary constriction (arrow) marking the adoral end of the ammonitella. **F.** Healed injury (arrow) on the early postembryonic shell.

AMMONITELLA: The ammonitella (embryonic shell) consists of the initial chamber and approximately two-thirds of a whorl (figs. 6, 7). The outer whorls of the ammonitella are covered with a tuberculate microornamentation, as previously described in Landman et al. (1996). In general, the tubercles are irregularly distributed, although some tubercles are arranged in rows along the ven-

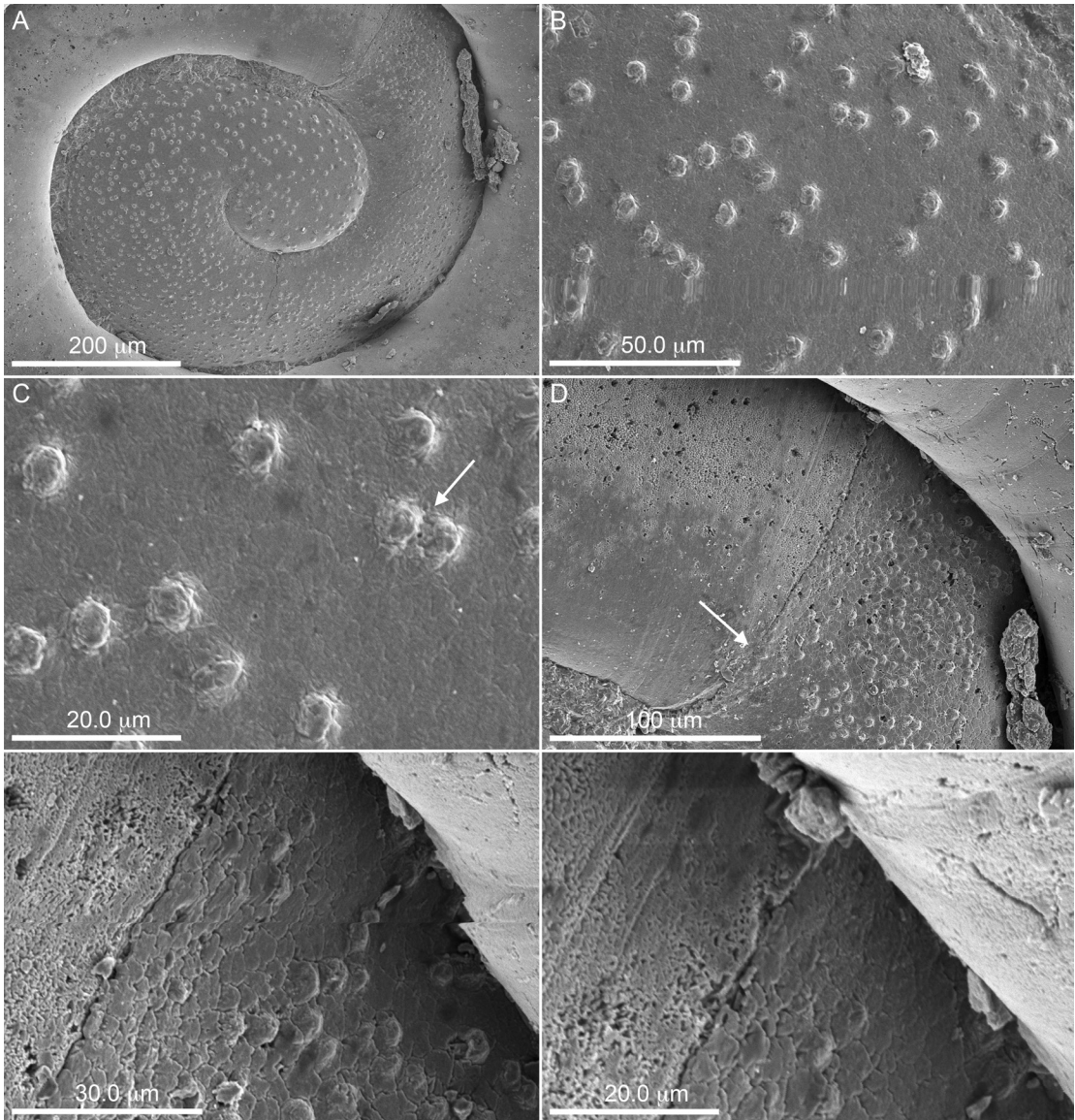


FIG. 7. Early whorls of *Hoploscaphites sargklofak*, n. sp. A–F. AMNH 63590, AMNH loc. 3278, Weston County, Wyoming. **A.** Overview of the tuberculate microornamentation on the ammonitella. **B.** Tuberculate microornamentation on the initial chamber. **C.** Close-up of the tubercles on the initial chamber showing their irregular distribution, with some tubercles closely spaced together (arrow). **D.** Overview of the primary constriction (arrow) marking the adoral end of the ammonitella. **E.** Close-up of the primary constriction showing the end of the ammonitella and the beginning of the postembryonic shell. **F.** The postembryonic shell is marked with growth lines.

trilateral margin. The postembryonic shell emerges from below the embryonic shell at the primary constriction. The postembryonic shell is marked with growth lines and healed injuries.

MACROCONCH DESCRIPTION: In the measured sample, LMAX averages 51.5 mm and ranges from 32.6 to 92.2 mm (fig. 8; table 1). The ratio of the size of the largest specimen to that of the smallest is 2.82. The ratio of the size of the next to largest specimen to that of the

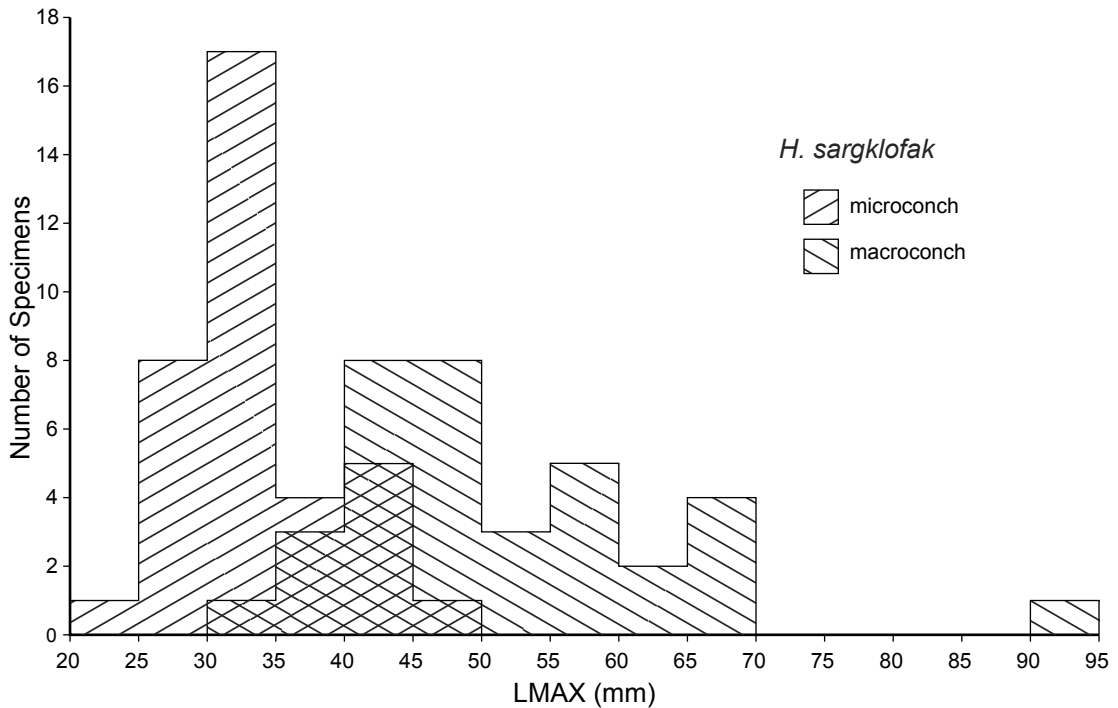


FIG. 8. Size-frequency histogram of *Hoploscaphites sargklofak*, n. sp., from the *Baculites grandis* Zone of the Pierre Shale, Bearpaw Shale, and Lewis Shale, based on the samples in tables 1 and 2.

smallest is 2.06. The specimens form a unimodal size distribution, with a peak at 40–50 mm, and a single outlier between 90–95 mm. As noted in other studies (Landman et al., 2010; Landman and Klofak, 2012), the size range is reduced in a sample from a single locality (AMNH loc. 3435). LMAX averages 42.9 mm and ranges from 38.0 to 45.5 mm at AMNH locality 3435; the ratio of the size of the largest specimen to that of the smallest is 1.20 (fig. 9).

Adults are slender with an oval to rounded outline in side view. LMAX/ H_s averages 2.09 and ranges from 1.89 to 2.43 (2.04 in the holotype). YPM 35642 (fig. 12M–P) is an example of an elongate form (LMAX/ H_s = 2.14) and USNM 605796 (fig. 11I–L) is an example of a more rounded form (LMAX/ H_s = 2.07).

The umbilicus is small and deep. The umbilical diameter averages 3.7 mm and ranges from 2.6 to 5.4 mm. UD/LMAX averages 0.07 and ranges from 0.05 to 0.14, reflecting the broad variation in relative umbilical diameter (fig. 7). Our collection contains two end-member morphotypes with transitional forms in between: (1) an openly umbilicate form, for example, AMNH 74374 (fig. 11E–H), with an umbilical bulge and (2) a more tightly coiled umbilicate form, for example, AMNH 64710 (fig. 15A–C), with a straight umbilical shoulder. The umbilical bulge usually extends several millimeters along the umbilical shoulder.

All specimens tend to be tightly coiled with no gap between the phragmocone and hook. LMAX/ H_p averages 2.78 and ranges from 2.59 to 3.11 (2.76 in the holotype). AMNH 90566 (fig. 16E–F) is an example of a tightly coiled specimen (LMAX/ H_p = 2.76) and YPM 35638 (fig. 12I–L) is an example of a more loosely coiled specimen (LMAX/ H_p = 2.93). The exposed

Table 1. Measurements of *Hoploscaphites sargklofak*, n. sp., macroconchs. See figure 4 for description of measurements. All measurements are in mm, except for apertural angle. * = holotype.

Specimen Number	Locality	LMAX	LMAX/ H _p	LMAX/ H _s	AA	UD	UD/ LMAX	W _p /H _p	W _s /H _s	W _H /H _H	V _s /H _s
AMNH 63556	3435	43.4	–	–	44.5	3.2	–	–	0.67	1.01	–
AMNH 64670	3278	69.0	2.59	2.02	39.0	4.3	0.06	0.64	–	–	–
AMNH 64679	3487	48.3	2.86	2.08	41.0	4.5	0.09	0.76	0.67	0.97	0.36
AMNH 64684	3487	38.4	2.82	2.10	38.0	4.3	0.11	0.71	0.66	0.92	0.36
AMNH 64710	3278	59.7	2.65	2.09	45.0	3.2	0.05	0.65	0.65	0.90	0.32
AMNH 74364	3728a	66.7	2.81	2.02	39.5	4.3	0.06	0.76	0.71	1.04	0.32
AMNH 74365	3728	66.8	2.75	1.89	53.5	3.3	0.05	0.84	0.69	1.06	0.31
AMNH 74366	3727	62.4	2.59	1.97	56.0	3.2	0.05	0.70	0.69	1.07	0.27
AMNH 74367	3728	56.2	2.71	2.07	48.0	3.4	0.06	0.83	0.72	0.89	0.35
AMNH 74374	3731	48.6	2.83	2.20	27.5	4.8	0.10	0.78	0.78	1.04	0.40
AMNH 90566	3435	42.8	2.76	–	34.5	3.2	0.07	0.70	–	0.95	–
AMNH 90567	3435	38.0	–	–	50.5	3.6	–	–	–	1.04	–
AMNH 90568	3435	–	–	–	42.0	3.4	–	–	0.74	0.97	–
AMNH 95769	3265	67.1	2.82	2.00	52.0	3.6	0.05	0.72	0.57	0.86	–
AMNH 100157	3487	92.2	2.68	2.02	–	4.3	0.05	0.67	0.67	0.87	0.29
BHI 4312	?	41.8	2.79	2.08	28.0	4.7	0.11	0.73	0.71	0.94	0.32
USNM 605785	D1986	40.5	2.96	2.14	41.0	3.6	0.09	0.85	0.73	1.08	0.39
USNM 605786	D11783	44.8	2.99	2.19	40.0	4.4	0.10	0.72	0.75	1.03	0.34
USNM 605788*	24312	54.3	2.76	2.04	39.5	3.5	0.06	0.70	0.68	0.95	0.33
USNM 605789	?	47.8	2.67	2.03	24.5	4.3	0.09	0.78	0.70	1.06	0.31
USNM 605790	24312	55.6	2.66	2.07	52.0	3.4	0.06	0.79	0.79	1.07	0.36
USNM 605792	D11783	60.5	2.67	2.02	46.5	3.5	0.06	0.71	0.71	0.96	0.36

Specimen Number	Locality	LMAX	LMAX/ H _p	LMAX/ H _s	AA	UD	UD/ LMAX	W _p /H _p	W _s /H _s	W _H /H _H	V _s /H _s
USNM 605796	D2118	44.1	2.77	2.07	26.5	4.7	0.11	0.72	0.64	0.92	–
USNM 605797	?	52.5	2.76	2.06	48.0	3.2	0.06	0.71	0.71	0.99	0.35
USNM 605798	D2118	40.8	2.74	2.13	37.0	3.2	0.08	0.70	0.70	0.95	0.39
USNM 605811	D1033	48.7	2.71	2.13	36.0	3.4	0.07	0.73	0.72	0.96	0.34
USNM 605787	D2118	48.7	–	–	–	2.6	0.05	–	–	–	–
USNM 605791	10768	44.2	3.01	2.43	–	5.0	0.11	0.93	0.80	–	0.44
USNM 605793	Crook Co., WY	58.4	2.65	2.10	59.0	2.7	0.05	0.70	0.72	1.05	0.32
USNM 605795	22114	46.1	2.74	–	39.0	3.3	0.07	0.72	–	1.04	–
USNM 605794	10768	50.2	2.82	2.07	45.0	2.7	0.05	0.75	0.65	0.99	0.32
USNM 605799	D6381	32.6	2.94	2.19	–	2.7	0.08	0.76	0.63	–	0.36
YPM 35637	A4768	38.6	3.11	2.06	41.0	5.4	0.14	0.85	0.73	1.06	0.36
YPM 35638	A4768	47.2	2.93	2.15	52.0	3.9	0.08	0.75	0.74	1.04	0.36
YPM 35639	A4768	44.4	2.74	2.07	41.0	2.7	0.06	0.75	0.74	1.13	0.36
YPM 35642	A4768	48.1	2.78	2.14	44.0	3.7	0.08	0.76	0.75	0.98	0.38
YPM 35643	A4768	37.4	2.88	2.17	56.5	2.6	0.07	0.75	0.69	0.95	0.38
YPM 35652	A4768	56.9	2.70	2.05	54.0	3.0	0.05	0.70	0.58	0.88	–
Average		51.5	2.78	2.09	43.0	3.7	0.07	0.74	0.70	0.99	0.35

phragmocone occupies approximately one-half whorl and terminates slightly above, at, or slightly below the line of maximum length. The body chamber consists of a short shaft and recurved hook totaling slightly more than one-half whorl. The apertural lip is flexuous with a deep constriction. The apertural angle averages 43.0° and ranges from 24.5 to 59.0° (39.5° in the holotype). The value of the apertural angle correlates with the relative size of the umbilicus, so that more openly umbilicate forms exhibit a lower apertural angle than less openly umbilicate forms (fig. 10). In addition, as in other scaphites, the value of the apertural angle correlates with the position of the base of the body chamber. In specimens in which the base of the body chamber occurs above the line of maximum length, the apertural angle is lower than in specimens in which it occurs below the line of maximum length.

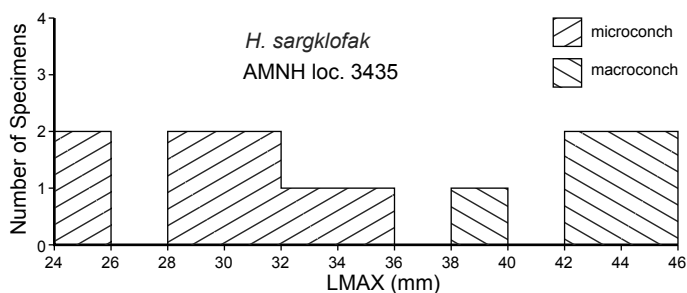


FIG. 9. Size-frequency histogram of *Hoploscaphites sargklofak*, n. sp., at a single locality (AMNH loc. 3435, *Baculites grandis* Zone, Pierre Shale, Meade County, South Dakota).

The whorl section of the phragmocone along the line of maximum length is compressed subquadrate with maximum whorl width at one-third whorl height. W_p/H_p averages 0.74 and ranges from 0.64 to 0.93 (0.70 in the holotype). The umbilical wall is steep and subvertical and the umbilical shoulder is sharply rounded. The flanks are nearly flat and subparallel and converge toward the venter starting at two-thirds whorl height. The ventrolateral shoulder is sharply rounded and the venter is nearly flat.

As the shell passes from the phragmocone into the body chamber, the whorl width increases markedly. It reaches its maximum value at the point of recurvature and diminishes slightly thereafter. Whorl height increases even more markedly during this transition and reaches its maximum value at midshaft. Thereafter, it diminishes to the point of recurvature and remains nearly the same up to the aperture. Because of these changes in whorl width and height, the whorl section at midshaft is only slightly more compressed than that along the line of maximum length. W_s/H_s averages 0.70 and ranges from 0.57 to 0.80 (0.68 in the holotype). V_s/H_s averages 0.35 and ranges from 0.27 to 0.44 (0.33 in the holotype). The intercostal whorl section is subovoid to subquadrate with maximum whorl width at one-quarter whorl height. The umbilical wall is steep and subvertical and the umbilical shoulder is sharply rounded. The inner flanks are very broadly rounded and the outer flanks are nearly flat and converge toward the venter. The ventrolateral shoulder is sharply rounded and the venter is nearly flat.

The whorl section at the point of recurvature is less compressed than that at midshaft, mainly due to a decrease in whorl height. W_H/H_H averages 0.99 and ranges from 0.86 to 1.13 (0.95 in the holotype). The intercostal whorl section at the point of recurvature is subovoid with maximum whorl width at one-quarter whorl height. The umbilical wall is slightly concave and the umbilical shoulder is sharply rounded. The flanks are broadly rounded and gently converge toward the venter.

At the point of exposure, ribs emerge at the umbilical seam and strengthen across the umbilical wall and shoulder. They are slightly prorsiradiate on the flanks. They are straight or, more rarely, weakly flexuous, bending slightly backward on the inner flanks, slightly forward on the midflanks, and slightly backward again on the outer flanks. The degree of flexuosity varies depending on the coarseness of the ornament. For example, in USNM 605785 (not figured) the ribs are coarse and straight and bear strong lateral tubercles, whereas in AMNH 74374 (fig. 11E-H) the ribs are finer and more flexuous and bear weaker lateral

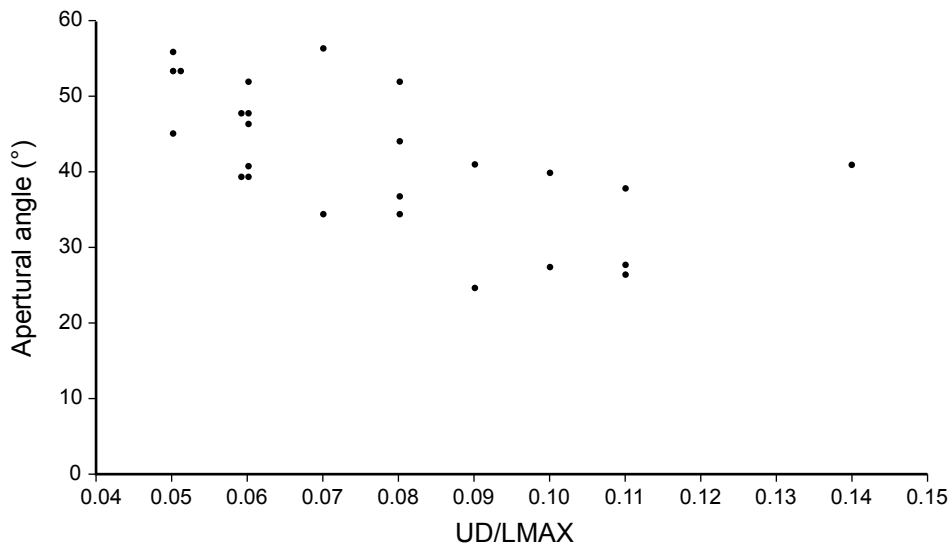


FIG. 10. Apertural angle versus UD/LMAX in macroconchs of *Hoploscaphites sargklofak*, n. sp. The apertural angle tends to be larger in specimens with relatively smaller umbilici.

tubercles. Lirae are present on the ribs and the interspaces between ribs. Intercalation and branching occur at one-third and two-thirds whorl height, corresponding to the sites of the umbilical bullae and lateral tubercles (if present), respectively. Ribs are uniformly strong on the venter, which they cross with a slight adoral projection. The rib density on the adapical part of the phragmocone ranges from 5 to 9 ribs/cm, with most values between 6 and 8 ribs/cm (7 ribs/cm in the holotype). The same pattern of ribbing persists onto the adoral part of the phragmocone. However, with the disappearance of the lateral tubercles at the adoral end of the phragmocone, the ribs on the outer flanks become weaker (in those forms in which lateral tubercles are present to begin with). The rib density on the phragmocone along the line of maximum length ranges from 5 to 9 ribs/cm, with most values between 6 and 8 ribs/cm (6 ribs/cm in the holotype).

On the body chamber, ribs arise at the umbilical seam and are rursiradiate on the umbilical wall and shoulder of the shaft, becoming more rectiradiate toward the aperture. They are prorsiradiate on the flanks and are straight to weakly flexuous. They swell and broaden on the midflanks, before disappearing toward the ventrolateral margin. Intercalation and branching occur at one-third and two-thirds whorl height. On well-preserved specimens, such as USNM 605792 (fig. 14A–C), the ribs on the outer flanks are fine and closely spaced, forming a broad band that extends to the aperture. These ribs are present only on the outer shell surface and are barely visible or absent on steinkerns such as AMNH 74365 (fig. 14G–I). The ribs on the venter of the shaft are faint in specimens that retain the outer shell wall, but are absent altogether in steinkerns. In the few specimens in which the ribs are visible, they show only a slight adoral projection. The rib density ranges from 7 to 13 ribs/cm with most values between 8 and 11 ribs/cm (7 ribs/cm in the holotype). Thus, the rib density shows a minimal increase from the adoral end of the phragmocone to the shaft.

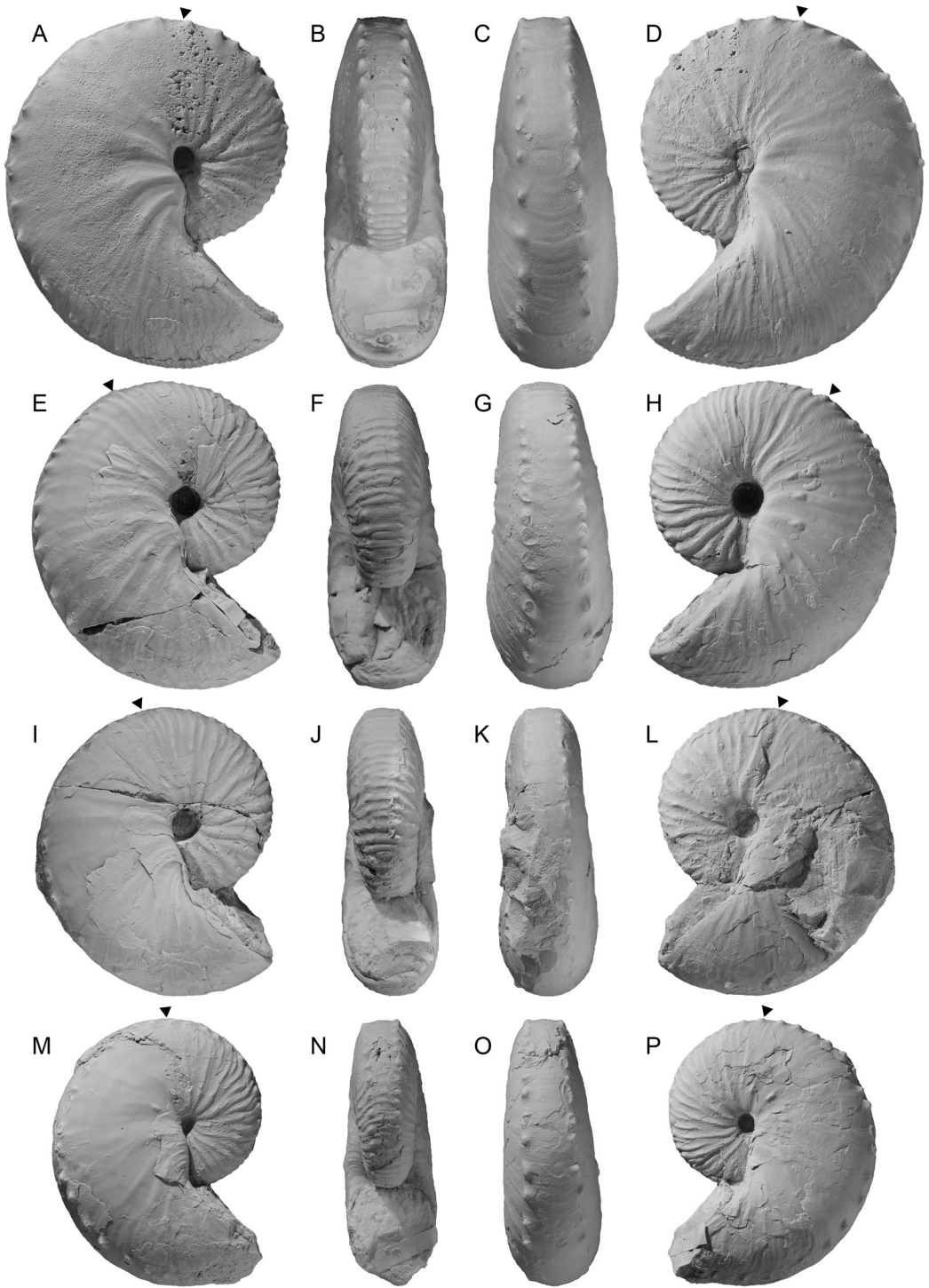
Table 2. Measurements of *Hoploscaphites sargklofak*, n. sp., microconchs. See figure 4 for description of measurements. All measurements are in mm.

Specimen Number	Locality	LMAX	LMAX/ H _p	UD	UD/ LMAX	W _p /H _p	W _s /H _s	W _H /H _H	V _s /H _s
AMNH 63547	3435	30.4	3.07	4.2	0.14	0.74	0.80	0.90	0.46
AMNH 63550	3435	27.7	3.08	4.9	0.18	0.73	–	0.89	–
AMNH 63552	3435	32.9	3.19	4.5	0.14	0.75	0.72	0.85	0.39
AMNH 63553	3435	31.9	3.22	4.5	0.14	0.86	0.77	0.90	0.46
AMNH 63557	3435	33.9	3.23	5.5	0.16	0.80	0.76	0.93	0.48
AMNH 63574	3194	28.2	3.00	2.7	0.10	0.68	0.63	0.86	0.34
AMNH 63579	3194	35.2	3.32	5.6	0.16	0.82	0.80	0.92	0.42
AMNH 63582	3278	32.1	2.89	4.0	0.12	0.75	0.81	0.96	0.46
AMNH 63583	3278	40.1	3.18	4.3	0.11	0.82	0.81	1.04	0.45
AMNH 63584	3278	–	–	4.4	–	0.81	0.79	0.95	0.43
AMNH 64607	3264	31.8	3.24	4.8	0.15	0.82	0.72	0.93	0.40
AMNH 64637	3487	29.8	3.39	4.5	0.15	0.83	0.75	0.88	0.40
AMNH 64651	3487	42.6	3.06	6.1	0.14	0.74	0.73	0.86	0.41
AMNH 64653	3487	24.7	3.21	4.1	0.17	0.79	0.68	0.80	0.38
AMNH 74292	3727	45.0	3.38	4.3	0.10	–	–	1.09	–
AMNH 74295	3728a	39.4	3.08	5.6	0.14	0.83	–	–	–
AMNH 74298	3728	41.4	3.37	3.6	0.09	0.80	0.69	0.92	0.43
AMNH 74300	3727	44.2	3.35	6.2	0.14	0.89	–	–	–
AMNH 74301	3728	37.3	2.89	5.0	0.13	0.70	0.71	0.88	0.35
AMNH 74303	3728	31.0	3.20	4.7	0.15	0.73	0.65	0.81	0.45
AMNH 74306	3728	34.5	3.29	5.4	0.16	–	–	0.94	0.47
AMNH 74307	3728a	31.2	3.71	5.7	0.18	0.85	0.72	0.91	0.34

Specimen Number	Locality	LMAX	LMAX/ H _p	UD	UD/ LMAX	W _p /H _p	W _s /H _s	W _H /H _H	V _s /H _s
AMNH 74310	3735	29.7	3.26	3.5	0.12	0.76	0.74	0.94	–
AMNH 74311	3728	30.8	3.21	4.3	0.14	0.90	0.74	–	0.46
AMNH 74312	3728a	32.4	3.24	4.2	0.13	0.80	–	–	–
AMNH 74313	3728a	31.9	3.29	5.4	0.17	0.85	0.80	0.94	0.53
AMNH 74314	3732	27.4	3.26	4.5	0.16	0.86	0.83	0.88	0.40
AMNH 74315	3727	34.7	2.99	5.1	0.15	0.72	0.64	–	–
AMNH 74316	3728a	30.1	3.42	5.3	0.18	0.93	0.94	1.04	–
AMNH 74317	3727	29.6	3.08	4.2	0.14	0.86	0.79	0.91	0.45
AMNH 74318	3732	34.1	3.07	4.4	0.13	0.87	0.81	0.96	0.36
AMNH 74319	3727	40.0	3.25	4.2	0.11	0.84	0.68	0.99	0.42
AMNH 74320	3732	27.8	3.34	4.8	0.18	0.84	0.81	0.90	0.50
USNM 605805	D396	31.2	3.06	4.6	0.15	0.72	0.76	0.91	0.38
USNM 605812	23625	49.3	3.16	3.8	0.08	0.77	0.79	0.94	0.42
YPM 35608	A4778	34.6	3.15	3.3	0.10	0.79	–	–	–
Average		33.8	3.21	4.6	0.14	0.80	0.76	0.92	0.43

The ribs become less flexuous on the adoral end of the shaft and hook. They are prorsiradiate with intercalation and branching at one-third and, especially, two-thirds whorl height. In the holotype, which is a steinkern with most of the outer shell wall missing, the ribs, which are faint at midshaft, become visible again on the adoral part of the shaft and hook. They are fine, closely spaced, and weakly flexuous, swinging slightly backward on the outer flanks and slightly forward again at the ventrolateral margin. Branching and intercalation occur at one-half whorl height. The rib density ranges from 9 to 20 ribs/cm with most values between 10 and 15 ribs/cm (12 ribs/cm in the holotype), indicating a marked increase in rib density from the shaft to the hook. Ribs cross the venter with a marked adoral projection and are much better developed than those on the shaft.

It is difficult to pin down the first appearance of umbilicolateral bullae or tubercles during ontogeny. In almost all specimens, the primary ribs at the point of exposure are strong and adorally concave at one-third whorl height, but usually what qualifies as a bulla or tubercle does not appear until near the adoral end of the phragmocone. Umbilicolateral bullae are



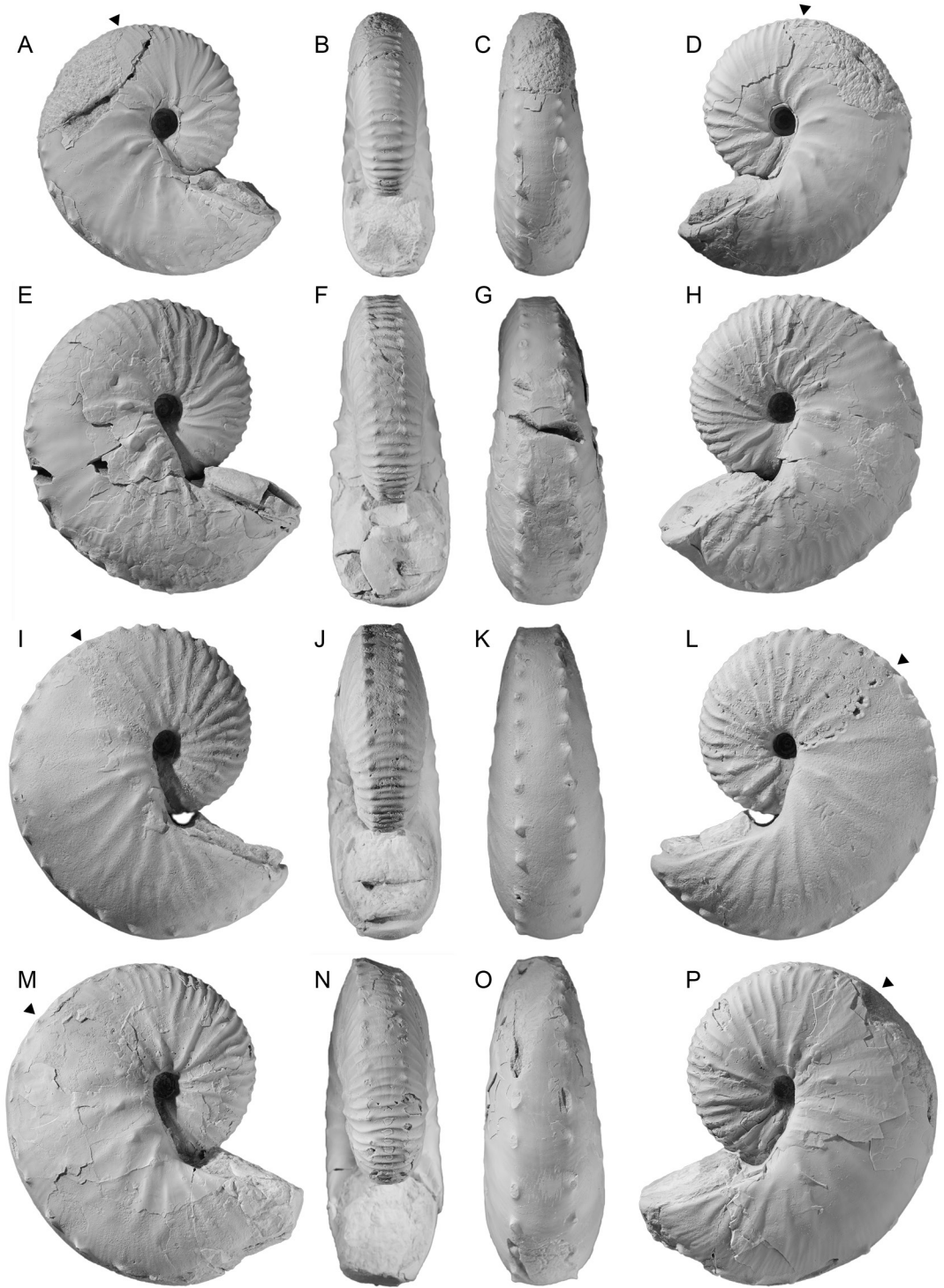
absent on the phragmocone of the holotype, but this is probably due to poor preservation. In contrast, in AMNH 74367 (fig. 13E, F) umbilicolateral bullae start midway on the phragmocone and become more tuberculate in an adoral direction. The maximum number of bullae or tubercles on the phragmocone in our measured sample is 6. The bullae are relatively evenly spaced with a maximum distance of 5 mm between them. One rib joins each bulla dorsally and one or two ribs branch from it ventrally.

Umbilicolateral bullae or tubercles are almost always present on the body chamber. They occur at one-quarter to one-third whorl height. They vary in strength depending on the coarseness of the ornament. In the holotype, which is a finely ornamented specimen, they appear as slightly raised areas 0.2 mm high, although this is probably an underestimate due to poor preservation. In AMNH 35639, a more coarsely ornamented specimen (not figured), the bullae are elevated into tubercles 0.8 mm high, which become more radially elongate toward the aperture. In USNM 605792 (fig. 14A–C), another coarsely ornamented specimen, the bullae almost develop into nodes at midshaft, one node of which is broader than the rib that bears it. These nodes are asymmetrical in cross section with a steep adapical face and a more gently sloping adoral face.

The number of umbilicolateral bullae or tubercles on the body chamber ranges from 4 to 7 (5 in the holotype), so that the total number of umbilicolateral bullae or tubercles on the entire exposed shell ranges from 5 to 12 (5 in the holotype). In general, the bullae are closely spaced on the adapical end of the shaft, more widely spaced at midshaft, and more closely spaced again on the hook. For example, in AMNH 74367 (fig. 13E, F) the distance between consecutive bullae starting at the base of the body chamber is 5.5, 5.5, 3.5, and 3.5 mm. A similar pattern appears in USNM 605792 (fig. 14A–C); the distance between consecutive bullae starting at the base of the body chamber is 1.5, 2.5, 3.5, 4.0, 3.5, 4.0, 4.0, and 3.0 mm. The holotype shows a slightly wider gap between bullae at midshaft. The distance between consecutive bullae in this specimen, starting at the base of the body chamber, is 4.5, 6.5, 4.5, and 4.5 mm. In general, one rib joins each bulla dorsally and two ribs branch from it ventrally; one or two ribs intercalate between bullae.

Ventrolateral tubercles are usually present at the point of exposure and are closely and evenly spaced. In the holotype, they occur on every rib or every other rib and become increasingly more widely spaced in an adoral direction, so that the distance between consecutive tubercles at the adoral end of the phragmocone is 4.5 mm. Similarly, in USNM 605785 (not figured), which is a small, coarsely ornamented specimen, the tubercles occur on every rib or every other rib, with a maximum distance of 2.5 mm between consecutive tubercles at the

←
 FIG. 11. *Hoploscaphites sargklofak*, n. sp., macroconchs. A–D. USNM 605788, holotype, USGS loc. 24312, McCone County, Montana. **A.** Right lateral; **B.** apertural; **C.** ventral; **D.** left lateral. E–H. AMNH 74374, AMNH loc. 3731, Niobrara County, Wyoming. **E.** Right lateral; **F.** apertural; **G.** ventral; **H.** left lateral. I–L. USNM 605796, paratype, USGS Mesozoic loc. D2118, Niobrara County, Wyoming. **I.** Right lateral; **J.** apertural; **K.** ventral; **L.** left lateral. M–P. USNM 605798, USGS Mesozoic loc. D2118, Niobrara County, Wyoming. **M.** Right lateral; **N.** apertural; **O.** ventral; **P.** left lateral. Specimens $\times 1$.



adoral end of the phragmocone. In AMNH 74367 (fig. 13E, F), the tubercles initially occur on every rib, but begin to appear on every other rib on the last adoral one-third of the phragmocone, with a maximum distance of 4 mm between consecutive tubercles at this point.

The number of ventrolateral tubercles on the phragmocone ranges from 12 to 24 with an average of 17 (14 tubercles in the holotype). The tubercles are conical in shape and change from slightly radially elongate at the point of exposure to slightly longitudinally elongate at the adoral end of the phragmocone. In our measured sample, the maximum height of a tubercle on the phragmocone ranges from 0.3–1.2 mm (1.0 mm in the holotype). One rib usually joins each ventrolateral tubercle dorsally and one to three ribs branch from it ventrally, looping between tubercles on opposite sides of the venter.

The presence of numerous, closely spaced ventrolateral tubercles on the body chamber, including the hook, is one of the distinctive features of this species. Ventrolateral tubercles are closely spaced on the adapical part of the shaft and become gradually more widely spaced in an adoral direction. They attain their maximum spacing on the adoral end of the shaft, and then become more closely spaced again on the hook. In the holotype, the distance between consecutive ventrolateral tubercles is 3.5 mm at the adapical end of the shaft, 5.5 mm at midshaft, 6.0 mm at the adoral end of the shaft near the point of recurvature, and 2.5 mm on the hook.

The total number of ventrolateral tubercles on the body chamber in our measured sample ranges from 14 to 32 with an average value of 20 (23 in the holotype). Therefore, the total number of ventrolateral tubercles on the entire exposed shell ranges from 32 to 47 with an average value of 38 (37 in the holotype). The ventrolateral tubercles are slightly clavate on the adoral end of the shaft where they attain their maximum height. The maximum height of the tubercles in the measured sample ranges from 0.5–1.5 mm (1.0 mm in the holotype). The tubercles become uniformly smaller on the hook and, in some instances, slightly radially elongate, as in the holotype (fig. 11A–D) and AMNH 74366 (fig. 15D–F).

Because of poor preservation, it is difficult to determine the relationship between the ventrolateral tubercles and the ribs at midshaft. In those specimens where the outer shell wall is preserved, it appears that 3 or 4 ribs join each tubercle dorsally and an equal number of ribs branch from it ventrally, looping between ventrolateral tubercles on opposite sides of the venter, as in AMNH 74367 (fig. 13E, F). The number of ribs that intercalate between consecutive tubercles depends on the position on the shaft. For example, in AMNH 74366 (fig. 15D–F) three ribs intercalate between consecutive tubercles at midshaft whereas eight ribs intercalate between consecutive tubercles on the adoral end of the shaft.

The presence of lateral tubercles on the adapical part of the phragmocone is common in this species, but not ubiquitous. They are present in approximately 25% of the specimens in our

FIG. 12. *Hoploscaphites sargklofak*, n. sp., macroconchs. A–D. AMNH 64684, AMNH loc. 3487, Weston County, Wyoming. A. Right lateral; B. apertural; C. ventral; D. left lateral. E–H. USNM 605786, USGS Mesozoic loc. D11783, Weston County, Wyoming. E. Right lateral; F. apertural; G. ventral; H. left lateral. I–L. YPM 35638, YPM loc. A4768, Niobrara Country, Wyoming. I. Right lateral; J. apertural; K. ventral; L. left lateral. M–P. YPM 35642, YPM loc. A4768. M. Right lateral; N. apertural; O. ventral; P. left lateral. Specimens $\times 1$.

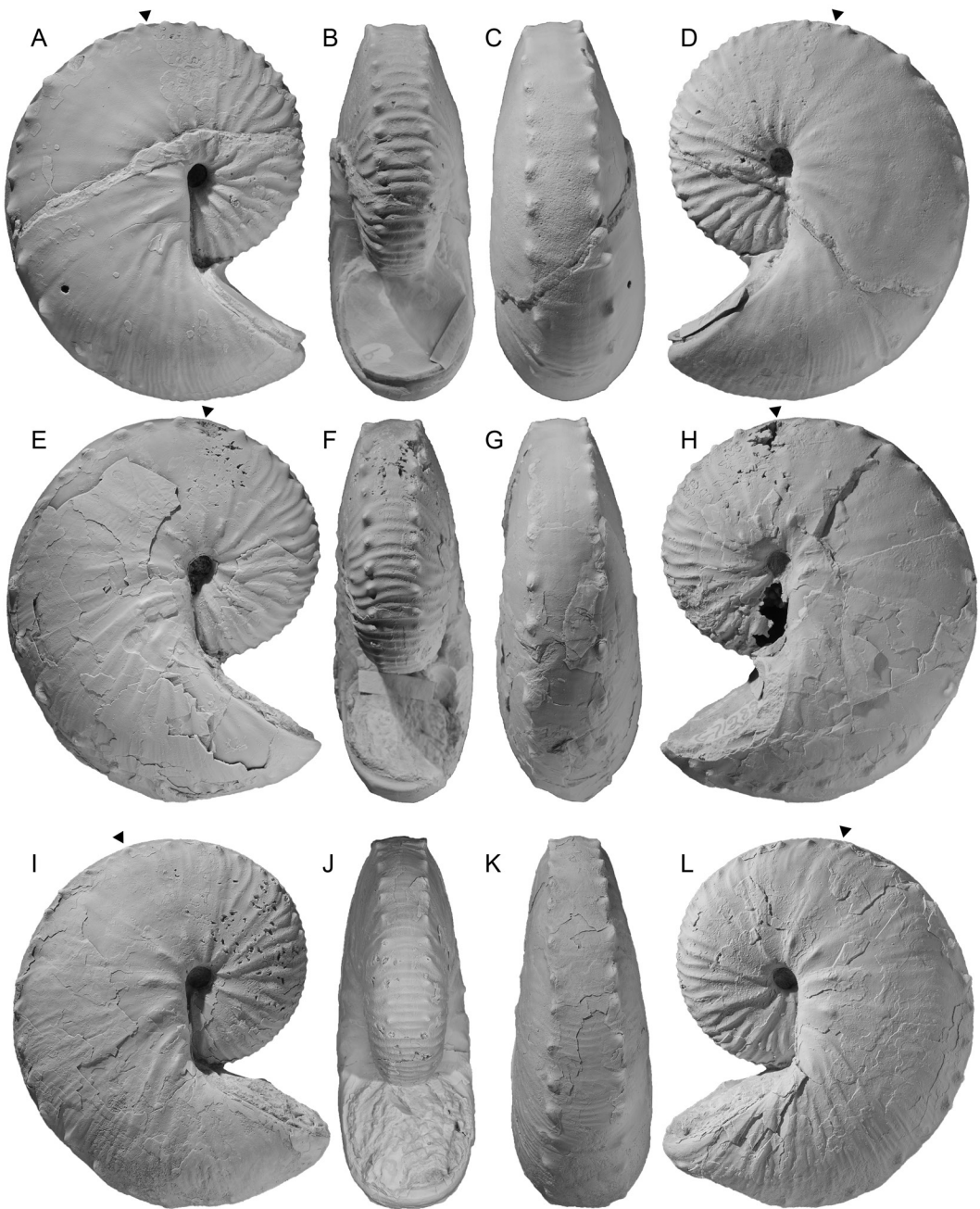


FIG. 13. *Hoploscaphites sargklofak*, n. sp., macroconchs. A–D. USNM 605790, USGS loc. 24312, McCone County, Montana. A. Right lateral; B. apertural; C. ventral; D. left lateral. E–H. AMNH 74367, AMNH loc. 3728, Niobrara County, Wyoming. E. Right lateral; F. apertural; G. ventral; H. left lateral. I–L. USNM 605797, locality unknown. I. Right lateral; J. apertural; K. ventral; L. left lateral. Specimens $\times 1$.

sample, not including the holotype. In some specimens, such as AMNH 74374 (fig. 11E–H), they appear as swellings at two-thirds whorl height. The ribs show a break in profile at this point but do not form distinct tubercles. In other specimens, a single or double row of tubercles appears at the point of exposure. For example, in YPM 35638 (fig. 12I–L), a single row of 10 lateral tubercles extends from the point of exposure to midway on the phragmocone. The tubercles occur at three-quarters whorl height and are not as strong as the ventrolateral tubercles. They are more or less evenly spaced and occur on every rib or every other rib. Similarly, in AMNH 74367 (fig. 13E, F), a single row of six lateral tubercles occurs on the adapical one-half of the phragmocone. In contrast, in USNM 605792 (fig. 14A–C), two rows of lateral tubercles are present. The outer row occurs at three-quarters whorl height and extends from the point of exposure to nearly the end of the phragmocone. It consists of eight tubercles, which are evenly spaced at distances of 2.5 mm on every other rib. An additional row of five tubercles occurs at two-thirds whorl height but is restricted to the adapical end of the phragmocone. These tubercles occur on the same ribs as the outer lateral tubercles but are weaker and more bullate.

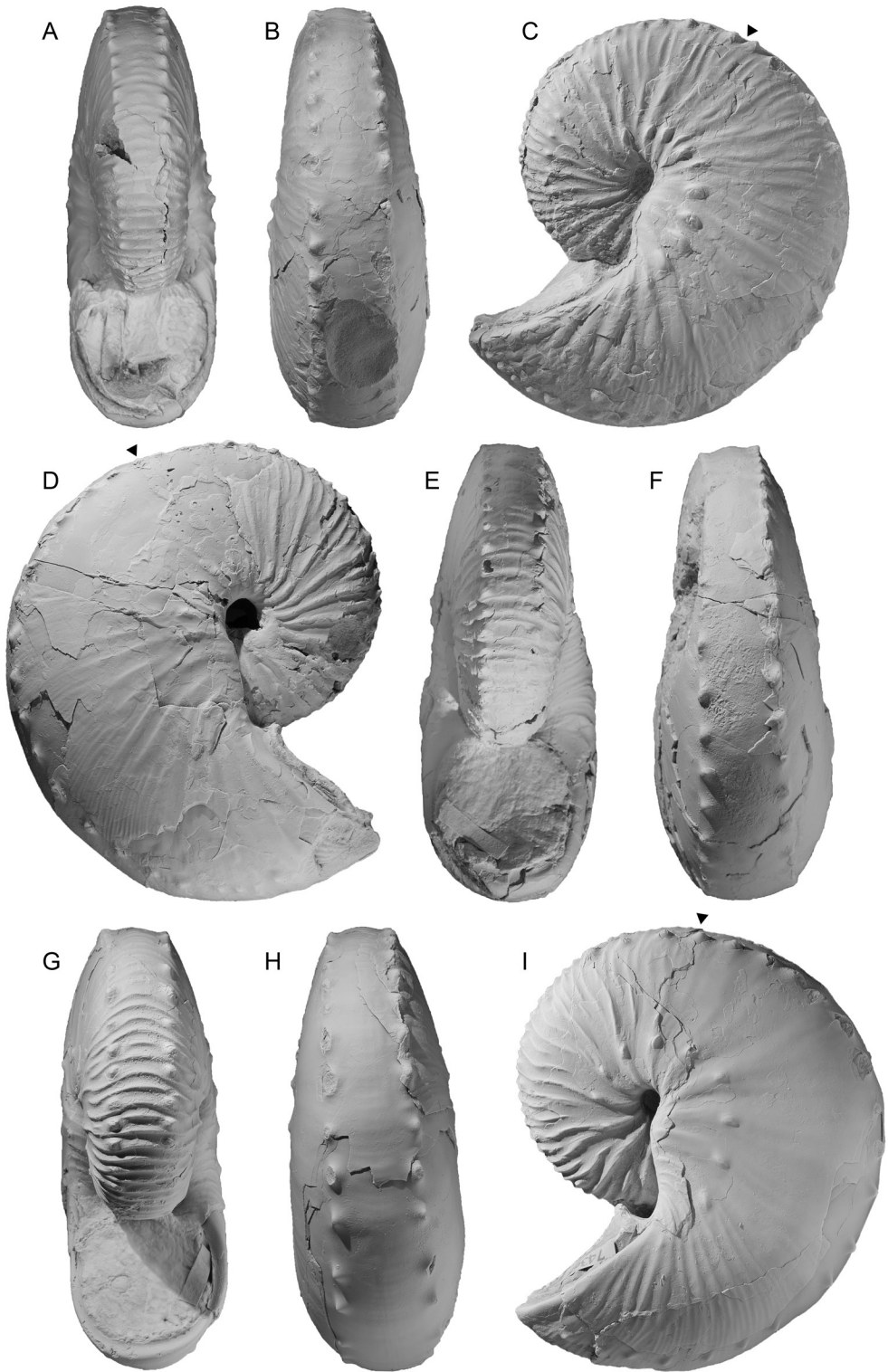
Lateral tubercles also occasionally appear on the hook. In USNM 605792 (fig. 14A–C), a single row of three lateral tubercles extends from near the point of recurvature to the aperture. The tubercles are slightly smaller than the ventrolateral tubercles and immediately adjacent to them. Similarly, in AMNH 90567 (fig. 16J–L), a single row of five lateral tubercles extends from the adoral end of the shaft to the aperture. They are unevenly spaced with a large gap of 10.5 mm between the two most adapical tubercles. In AMNH 63556 (fig. 16A–D), a single row of three lateral tubercles also extends from the adoral end of the shaft to the aperture. An additional inner lateral tubercle is present near the aperture, giving the impression that the tubercles are randomly scattered on the shell.

The suture is deeply incised, with a broad, asymmetrically bifid first lateral saddle (E/L) and a narrow, symmetrically to asymmetrically bifid first lateral lobe (L) (fig. 17).

MICROCONCH DESCRIPTION: The most notable features of the microconchs are the relatively large umbilicus, little or no gap between the phragmocone and hook, subquadrate whorl section of the shaft with fairly flat flanks, numerous, closely spaced ventrolateral tubercles on the phragmocone and body chamber, and umbilicolateral bullae on the body chamber.

LMAX averages 33.8 mm and ranges from 24.7 to 49.3 mm (fig. 8; table 2). The average size of microconchs is 0.66 that of macroconchs. As in macroconchs, the size distribution is unimodal, with a peak between 30–35 mm. The few larger microconchs such as USNM 605812 (fig. 19R–T) presumably correspond to the few larger macroconchs in our collection such as AMNH 74366 (fig. 15D–F). The ratio of the average size of microconchs to that of macroconchs at a single locality (AMNH loc. 3435) is 0.69.

Microconchs are oval to nearly circular in lateral view. The phragmocone occupies slightly more than one-half whorl and usually terminates just above the line of maximum length. Specimens are tightly coiled with a small gap between the phragmocone and hook. LMAX/H_p averages 3.21 and ranges from 2.89 to 3.71. AMNH 74316 (fig. 18U–X) is an example of a loosely coiled specimen (LMAX/H_p = 3.42) and AMNH 74315 (fig. 19E, F) is an example of a tightly coiled specimen (LMAX/H_p = 2.99).



The umbilical seam of the shaft follows the curve of the venter. The body chamber occupies slightly more than one-half whorl and terminates in a constriction at the aperture. The umbilicus, as noted, is relatively large. $UD/LMAX$ averages 0.14 and ranges from 0.08 to 0.18. The early whorls are well exposed in most specimens. For example, in AMNH 74313 (fig. 19A–D) all the whorls, including the ammonitella, are visible.

The whorl section along the line of maximum length is compressed subquadrate. W_p/H_p averages 0.80 and ranges from 0.68 to 1.11. The umbilical wall is nearly vertical and the umbilical shoulder is abruptly rounded. The flanks are subparallel and broadly rounded to flat. Maximum width occurs at one-quarter whorl height. The ventrolateral shoulder is abruptly rounded and the venter is broadly rounded to flat.

Whorl width increases gradually from the phragmocone into the body chamber and reaches its maximum value at the point of recurvature. Whorl height also increases gradually from the phragmocone into the body chamber and attains its maximum value at approximately the adapical part of the shaft. Thereafter, it decreases slightly to the aperture.

The whorl section at midshaft is compressed subquadrate with maximum width at one-quarter whorl height. W_s/H_s averages 0.76 and ranges from 0.63 to 0.94. The umbilical wall is steep and the umbilical shoulder slopes gently outward. The flanks are broadly rounded to flat and converge toward the ventrolateral margin. The ventrolateral shoulder is abruptly rounded and the venter is nearly flat.

The whorl section at the point of recurvature is more ovate than that at midshaft. W_H/H_H averages 0.92 and ranges from 0.80 to 1.09. The umbilical wall is broad and slopes gently outward to the umbilical shoulder. The flanks are broadly rounded with maximum width at one-quarter whorl height. The venter is broadly rounded except in those specimens that retain ventrolateral tubercles on the hook, such as AMNH 74319 (fig. 19O–Q).

At the point of exposure, ribs cross the umbilical wall of the phragmocone slightly rursiradiate. They swing gently backward and then forward on the inner one-third of the flanks, forming a weak adoral concavity. They then swing slightly forward and then backward again on the outer two-thirds of the flanks, forming a weak adoral convexity. The degree of flexuosity diminishes toward the base of the body chamber. On the adapical end of the phragmocone, the ribs strengthen at three-quarters whorl height, and sometimes bear a row of lateral tubercles. Intercalation and branching occur at one-third and, especially, three-quarters whorl height. Ribs are uniformly strong on the venter, which they cross with only a slight forward projection. They are relatively closely spaced with an average of 8 ribs/cm on both the adapical and adoral parts of the phragmocone.

Ribs are prorsiradiate and slightly flexuous on the shaft. They swing slightly backward on the inner flanks, slightly forward on the midflanks, and slightly backward again on the outer flanks. The ribs on the shaft are not as strong as those on the phragmocone. Intercalation and

FIG. 14. *Hoploscaphites sargklofak*, n. sp., macroconchs. A–C. USNM 605792, paratype, USGS Mesozoic loc. D11783, Weston County, Wyoming. A. Apertural; B. ventral; C. left lateral. D–F. AMNH 74364, AMNH loc. 3728a, Niobrara County, Wyoming. D. Right lateral; E. apertural; F. ventral. G–I. AMNH 74365, paratype, AMNH loc. 3728, Niobrara County, Wyoming. G. Apertural; H. ventral; I. left lateral. Specimens $\times 1$.

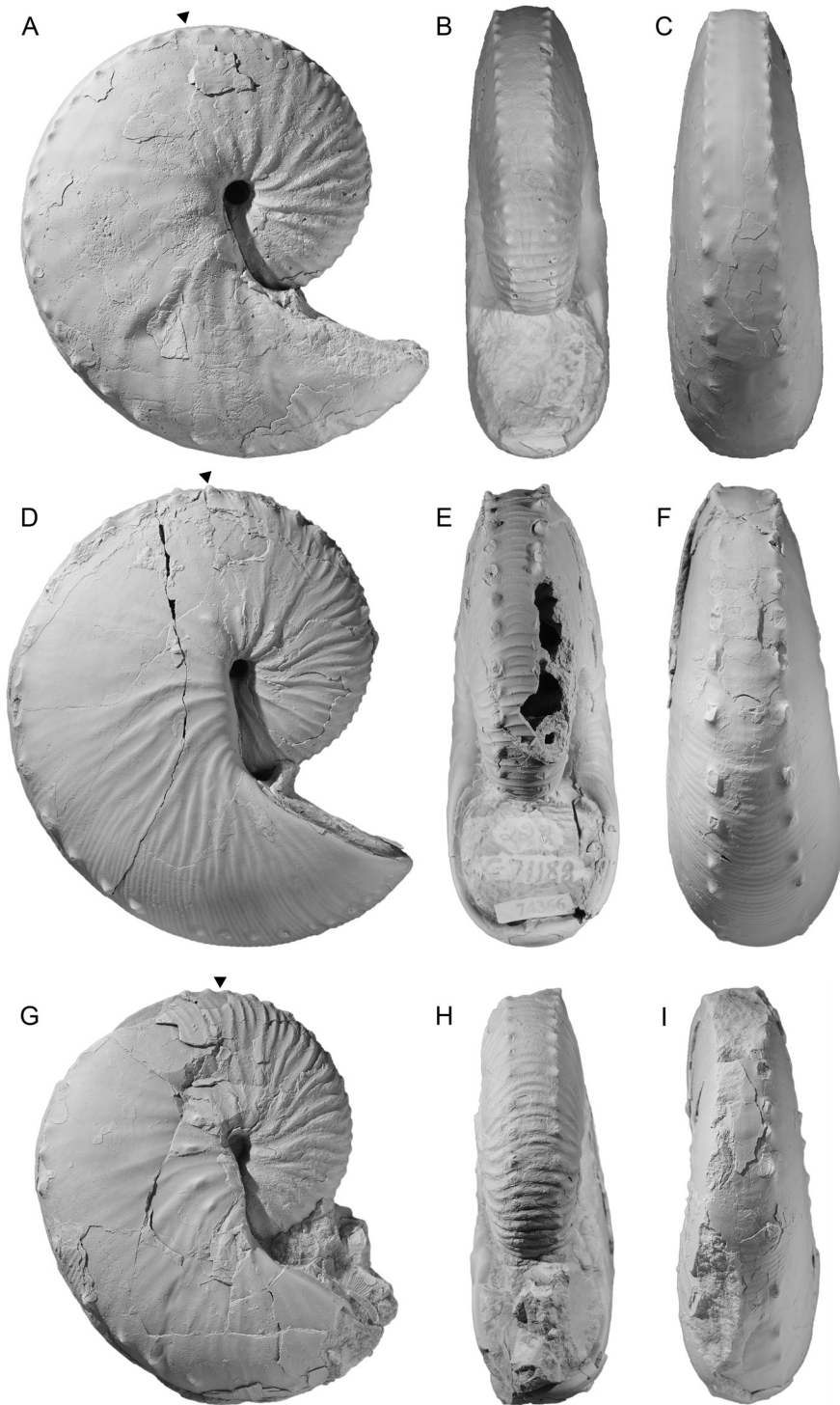


FIG. 15. *Hoploscaphites sargklofak*, n. sp., macroconchs. A–C. AMNH 64710, AMNH loc. 3278, Weston County, Wyoming. **A.** Right lateral; **B.** apertural; **C.** ventral. D–F. AMNH 74366, paratype, AMNH loc. 3727, Niobrara County, Wyoming. **D.** Right lateral; **E.** apertural; **F.** ventral. G–I. YPM 35652, YPM loc. A4768, Niobrara County, Wyoming. **G.** Right lateral; **H.** apertural; **I.** ventral. Specimens $\times 1$.

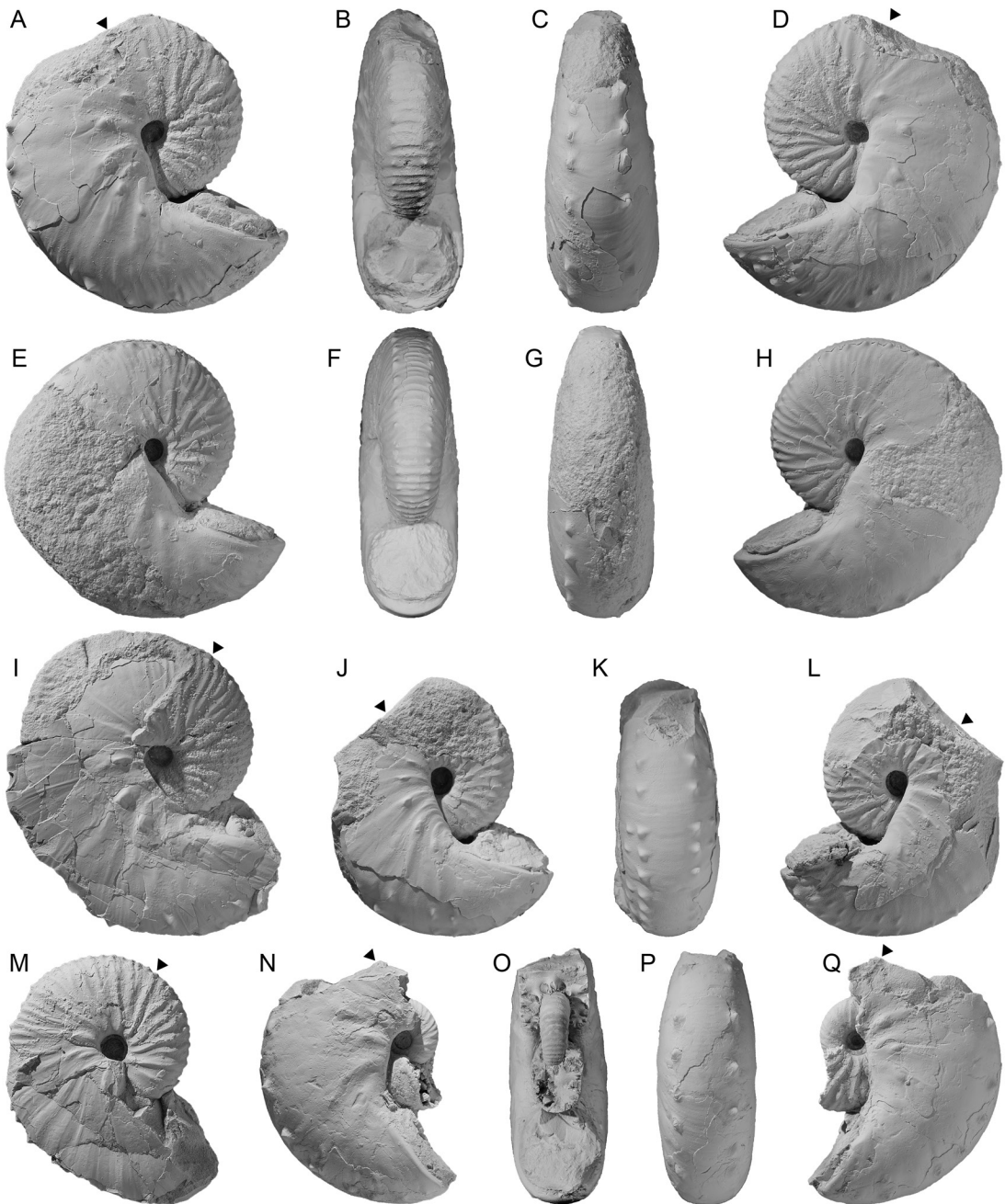


FIG. 16. *Hoploscaphites sargklofak*, n. sp., macroconchs, single concretion, AMNH loc. 3435, Meade County, South Dakota. A–D. AMNH 63556. A. Right lateral; B. apertural; C. ventral; D. left lateral. E–H. AMNH 90566. E. Right lateral; F. apertural; G. ventral; H. left lateral. I. AMNH 63560, right lateral. J–L. AMNH 90567. J. Right lateral; K. ventral; L. left lateral. M. AMNH 63554, right lateral. N–Q. AMNH 90568. N. Right lateral; O. apertural; P. ventral; Q. left lateral. Specimens $\times 1$.

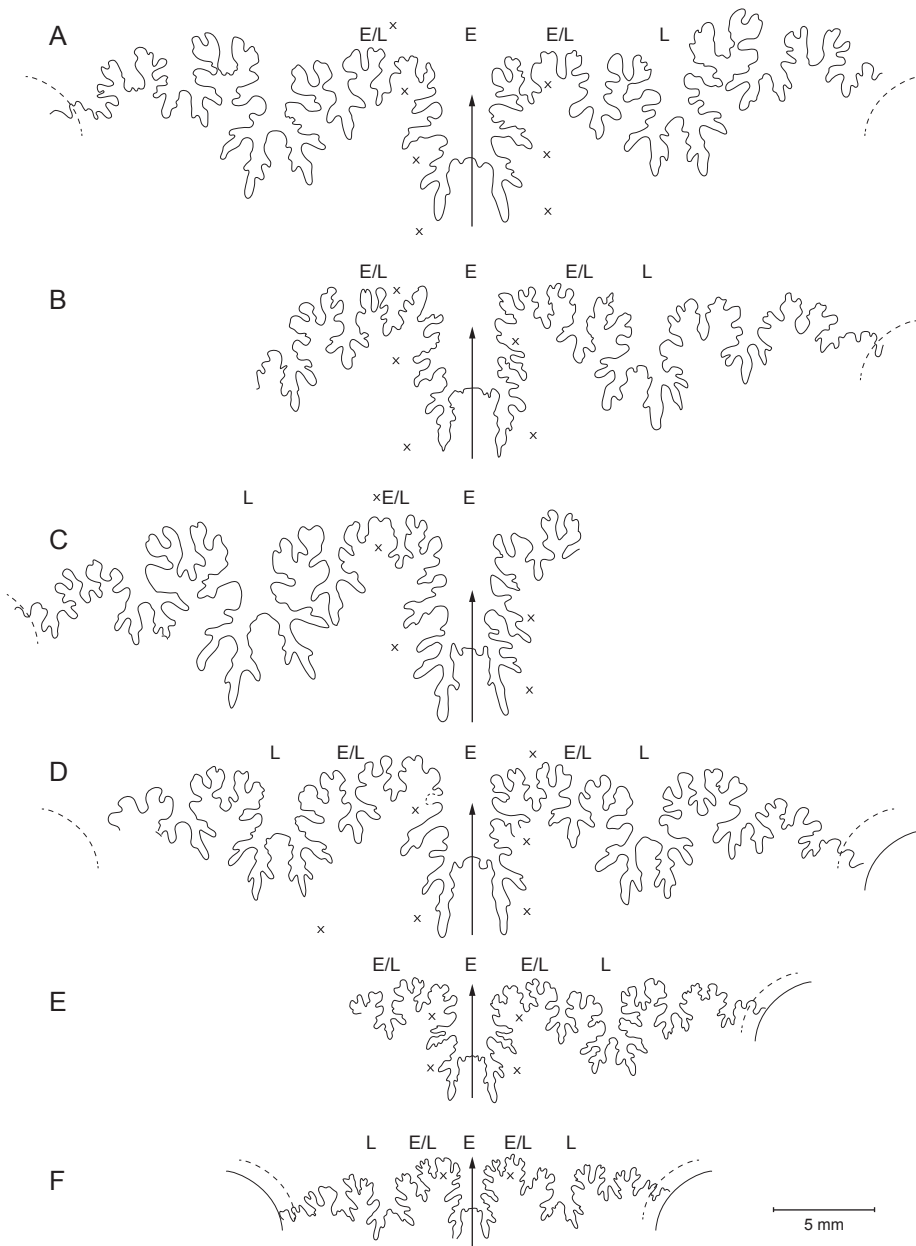


FIG. 17. *Hoploscaphites sargklofak*, n. sp., sutures. **A.** AMNH 74367, macroconch, fourth suture from the last, AMNH loc. 3728, Niobrara County, Wyoming. **B.** USNM 605788, macroconch, holotype, third suture from the last, USGS loc. 24312, McCone County, Montana. **C.** AMNH 71839, macroconch of closely related undescribed species, third suture from the last, *Baculites baculus* Zone, Bearpaw Shale, Dawson County, Montana. **D.** USNM 605812, microconch, paratype, third suture from the last, USGS loc. 23625, Richland County, Montana. **E.** AMNH 74319, microconch, paratype, third suture from the last, AMNH loc. 3727, Niobrara County, Wyoming. **F.** AMNH 74316, microconch, paratype, fourth suture from the last, AMNH loc. 3728a, Niobrara County, Wyoming. Abbreviations: x, tubercle; E, ventral lobe; E/L, first lateral saddle between ventral and lateral lobe; L, lateral lobe.

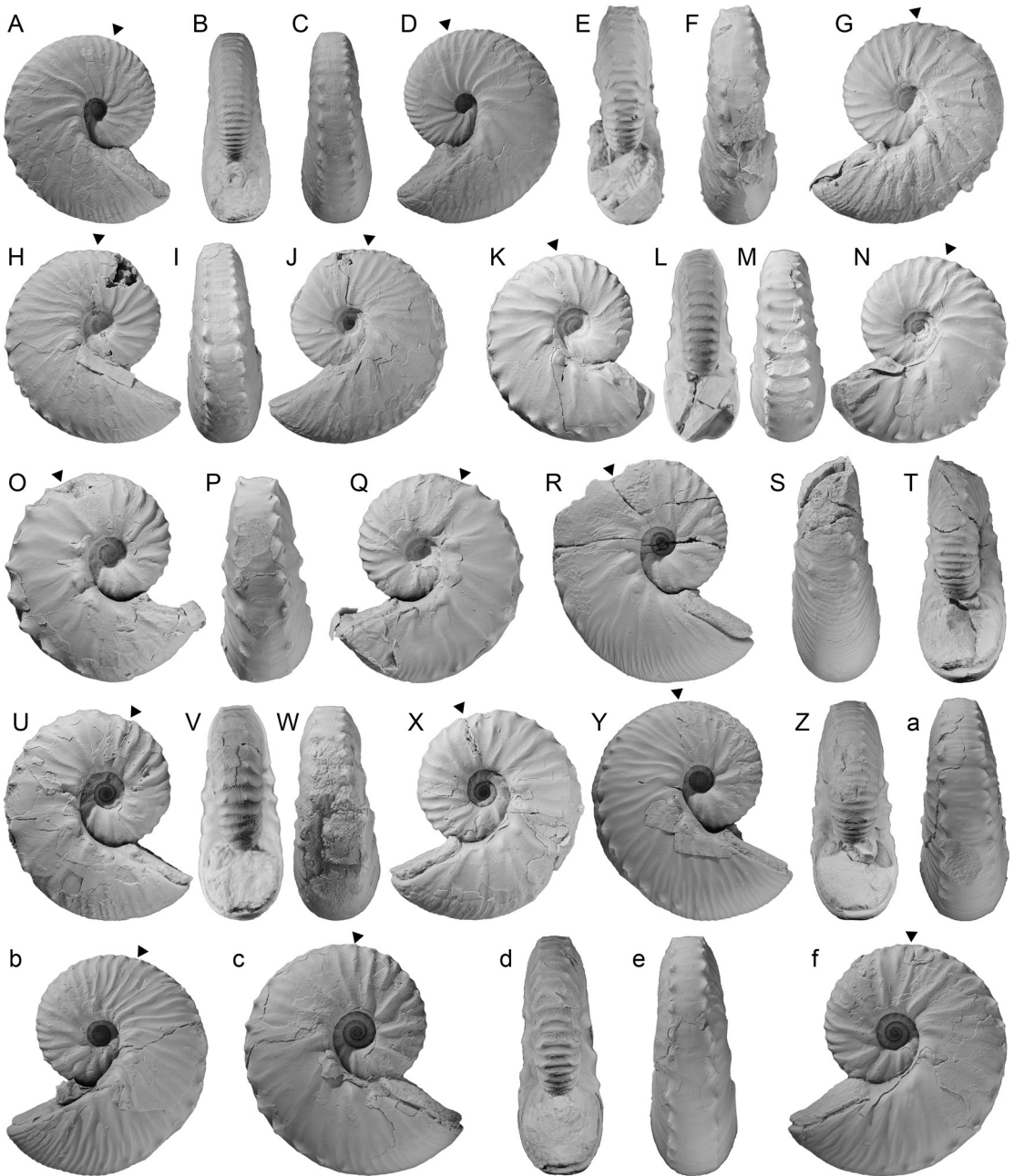


FIG. 18. *Hoploscaphites sargklofak*, n. sp., microconchs. A–D. AMNH 63574, AMNH loc. 3194, Weston County, Wyoming. A. Right lateral; B. apertural; C. ventral; D. left lateral. E–G. AMNH 74312, AMNH loc. 3728a, Niobrara County, Wyoming. E. Apertural; F. ventral; G. left lateral. H–J. AMNH 74314, AMNH loc. 3732, Niobrara County, Wyoming. H. Right lateral; I. ventral; J. left lateral. K–N. AMNH 74320, AMNH loc. 3728, Niobrara County, Wyoming. K. Right lateral; L. apertural; M. ventral; N. left lateral. O–Q. AMNH 74311, AMNH loc. 3728, Niobrara County, Wyoming. O. Right lateral; P. ventral; Q. left lateral. R–T. AMNH 63584, AMNH loc. 3278, Weston County, Wyoming. R. Right lateral; S. ventral; T. apertural. U–X. AMNH 74316, paratype, AMNH loc. 3728a, Niobrara County, Wyoming. U. Right lateral; V. apertural; W. ventral; X. left lateral. Y–b. AMNH 63582, AMNH loc. 3278, Weston County, Wyoming. Y. Right lateral; Z. apertural; a. ventral; b. left lateral. c–f. AMNH 63579, AMNH loc. 3194, Weston County, Wyoming. c. Right lateral; d. apertural; e. ventral; f. left lateral. Specimens $\times 1$.

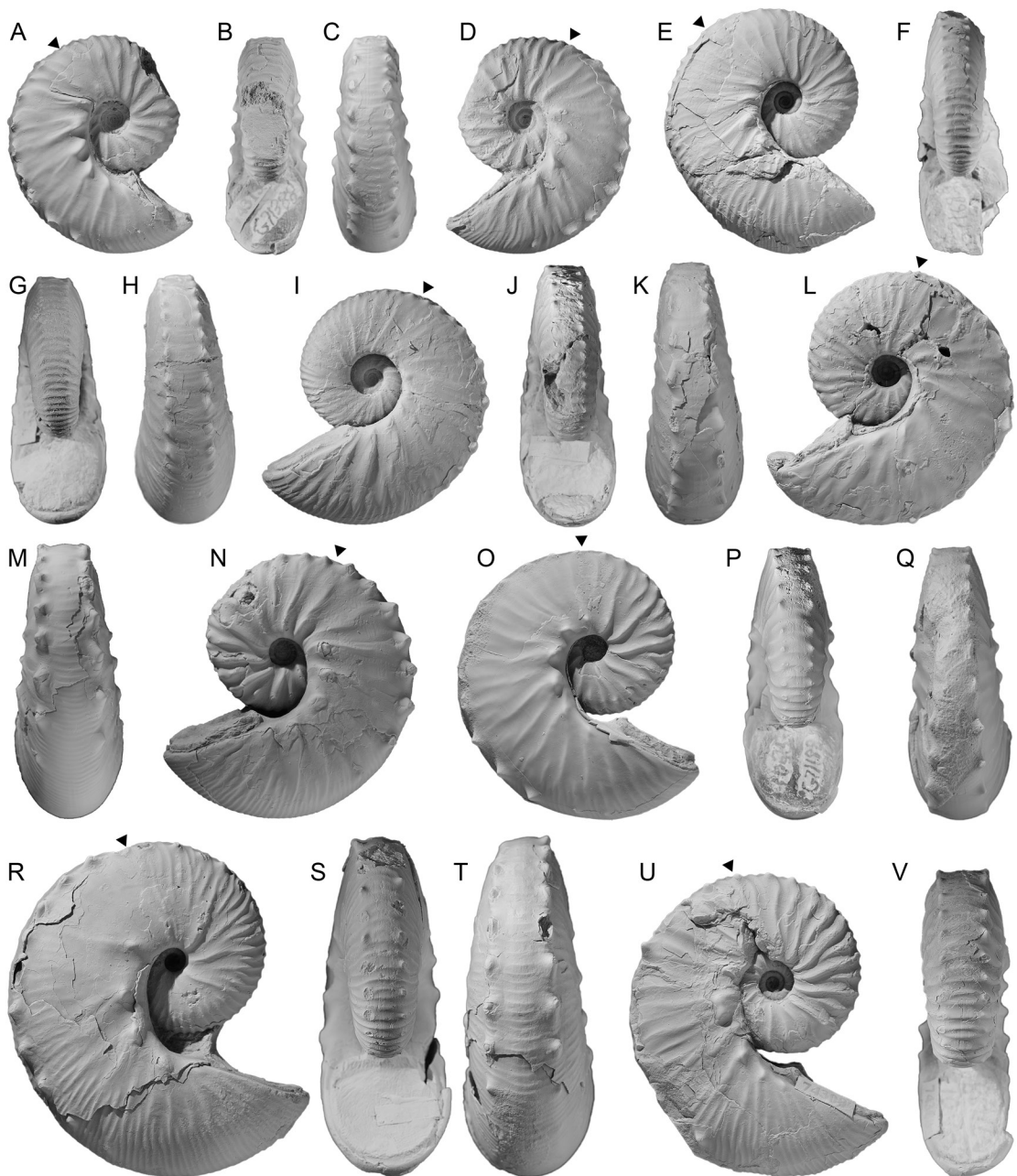


FIG. 19. *Hoploscaphites sargklofak*, n. sp., microconchs. A–D. AMNH 74313, AMNH loc. 3728a, Niobrara County, Wyoming. A. Right lateral; B. apertural; C. ventral; D. left lateral. E, F. AMNH 74315, AMNH loc. 3727, Niobrara County, Wyoming. E. Right lateral; F. apertural. G–I. AMNH 74318, AMNH loc. 3732, Niobrara County, Wyoming. G. Apertural; H. ventral; I. left lateral. J–L. AMNH 74301, AMNH loc. 3728, Niobrara County, Wyoming. J. Apertural; K. ventral; L. left lateral. M, N. AMNH 63583, AMNH loc. 3278, Weston County, Wyoming. M. Ventral; N. left lateral. O–Q. AMNH 74319, paratype, AMNH loc. 3728, Niobrara County, Wyoming. O. Right lateral; P. apertural; Q. ventral. R–T. USNM 605812, paratype, USGS Mesozoic loc. 23625, Richland County, Montana. R. Right lateral; S. apertural; T. ventral. U, V. AMNH 74300, AMNH loc. 3727, Niobrara County, Wyoming. U. Right lateral; V. apertural. Specimens $\times 1$.

branching occur at one-quarter and two-thirds whorl height. The ribs on the venter are usually poorly preserved, but in the few specimens in which they are visible, they show only a slight forward projection. The ribs are slightly more closely spaced on the shaft than those on the phragmocone, with an average of 9 ribs/cm.

Ribs are prorsiradiate on the hook. They are straight or show a broad adoral convexity on the midflanks, bending slightly backward and forward again at the ventrolateral shoulder. Inter-calculation and branching occur at one-half to two-thirds whorl height. In some specimens such as USNM 605812 (fig. 19R–T), the ribs on the hook are more prominent than those on the shaft. Ribs cross the venter with a marked forward projection. They are uniformly strong and more or less evenly spaced. The rib density ranges from 10 to 18 ribs/cm, indicating a substantial increase in rib density from the shaft to the hook.

Umbilicolateral tubercles or bullae are absent on the phragmocone in one-half of our specimens. In these specimens, the ribs are stronger and show a slight adoral concavity in this area. In the other one-half of our specimens, umbilicolateral bullae appear near the adoral end of the phragmocone. For example, in AMNH 74316 (fig. 18U–X), a small, but coarsely ornamented specimen (31.8 mm in diameter), and in USNM 605812 (fig. 19R–T), a large, but finely ornamented specimen (49.9 mm in diameter), two umbilicolateral bullae each appear at the adoral end of the phragmocone. The distance between consecutive bullae in each of these specimens is 2.5 and 5.0 mm, respectively.

In contrast, all the specimens in our sample exhibit umbilicolateral bullae on the body chamber. The bullae are evenly spaced and usually persist up to the aperture. The distance between consecutive bullae at midshaft ranges from 2.5–6.0 mm, e.g., 3.5, 6.0, and 3.0 mm in AMNH 74314 (fig. 18H–J), USNM 605812 (fig. 19R–T), and AMNH 74301 (fig. 19J–L), respectively. The number of umbilicolateral bullae on the body chamber in our sample ranges from 5 to 8, e.g., 5, 5, and 7 in AMNH 74314 (fig. 18H–J), USNM 605812 (fig. 19R–T), and AMNH 74301 (fig. 19J–L), respectively. In many specimens, the shape of the bulla changes during ontogeny. As shown in USNM 605812 (fig. 19R–T), the bullae are elongate on the adapical end of the shaft, tuberculate on the midshaft, and nodate on the adoral part of the shaft and hook. The nodes attain a height of 1 mm and display a steeply sloping adapical face and a more gently sloping adoral face. In most specimens, the height of the tubercle or bulla ranges from 0.4–0.8 mm. In general, one rib joins an umbilicolateral tubercle dorsally and two or three ribs branch from it ventrally.

Ventrolateral tubercles are present on the phragmocone beginning near the point of exposure. In general, they are evenly spaced, with a maximum distance of 2–4 mm between consecutive tubercles at the adoral end of the phragmocone. One or two ribs loop between ventrolateral tubercles on either side of the venter, with an occasional nontuberculate rib in between, as in AMNH 74300 (fig. 19U, V). A total of 8–13 ventrolateral tubercles are present on the exposed phragmocone. They develop a more conical shape toward the base of the body chamber, with a maximum height of 0.3–1 mm.

Ventrolateral tubercles are present on the body chamber and generally conform to the following pattern: closely spaced on the adapical part of the shaft, gradually becoming more widely spaced toward the midshaft. They attain their maximum spacing on the adoral part of the shaft, after which they generally disappear. If they persist onto the hook, they become

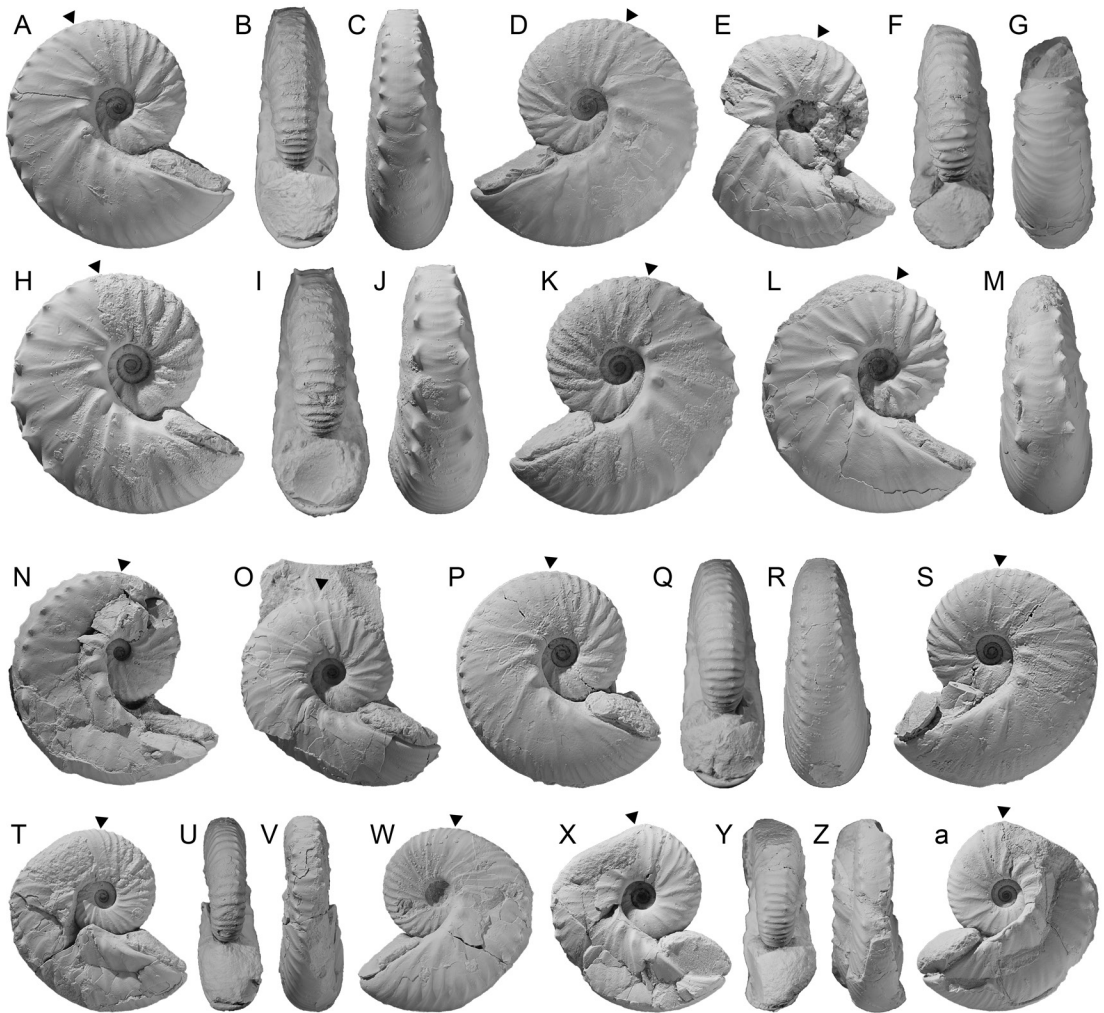


FIG. 20. *Hoploscaphites sargklofak*, n. sp., microconchs, single concretion, same as figure 16, AMNH loc. 3435, Meade County, South Dakota. A–D. AMNH 63552. A. Right lateral; B. apertural; C. ventral; D. left lateral. E–G. AMNH 63550. E. Right lateral; F. apertural; G. ventral. H–K. AMNH 63557. H. Right lateral; I. apertural; J. ventral; K. left lateral. L, M. AMNH 63553. L. Right lateral; M. ventral. N. AMNH 63555, right lateral. O. AMNH 63566, right lateral. P–S. AMNH 63547. P. Right lateral; Q. apertural; R. ventral; S. left lateral. T–W. AMNH 63558. T. Right lateral; U. apertural; V. ventral; W. left lateral. X–a. AMNH 63569. X. Right lateral; Y. apertural; Z. ventral; a. left lateral. Specimens $\times 1$.

more closely spaced again. Descriptions of three specimens help flesh out these patterns. In AMNH 74311 (fig. 18O–Q) the distance between consecutive tubercles is 4.0 mm on the adapical part of the shaft, 5.0 mm on the midshaft, 6.5 mm on the adoral part of the shaft, and 3.5 mm on the hook. In AMNH 74319 (fig. 19O–Q) the distance between consecutive tubercles is 4.0 mm on the adapical part of the shaft, 6.0 mm on the midshaft, 7.0 mm on the adoral part of the shaft, and 3.0 mm on the hook. In AMNH 74313 (fig. 19A–D) the distance between consecutive tubercles is 4.5 mm on the adapical part of the shaft, 5.5 mm on the midshaft, and 6.0 mm on the adoral part of the shaft, after which the tubercles disap-

pear. The maximum distance between consecutive tubercles at midshaft in our sample ranges from 2.5 to 6.0 mm.

The relationship between ribs and ventrolateral tubercles on the body chamber is difficult to determine because the ribs on the venter of the shaft are generally poorly preserved. In specimens in which the ribs are visible, two or three ribs loop between ventrolateral tubercles on either side of the venter with one or two nontuberculate ribs in between. This produces a succession of highs and lows on the venter, with the highs constituting the cluster of ribs that loop between tubercles and the lows constituting the nontuberculate ribs in between. The number of ventrolateral tubercles on the body chamber in our measured sample ranges from 9 to 16. Thus, the total number of ventrolateral tubercles on the exposed shell ranges from 21 to 28.

Ventrolateral tubercles become increasingly clavate toward the adoral end of the shaft where they reach their maximum height (0.4–1.4 mm in our sample). They exhibit a steeply sloping adapical face and a more gently sloping adoral face. In those specimens in which the ventrolateral tubercles continue onto the hook, they become smaller and more bullate.

Lateral tubercles are present only in 50% of the specimens in our sample. Of these, 20% show incipient tubercles, and 30% well-developed tubercles. Incipient tubercles consist of rib swellings that are not well enough defined to be called bullae or tubercles. For example, in AMNH 74316 (fig. 18U–X) a row of incipient tubercles appear at two-thirds whorl height on the adoral end of the phragmocone. In contrast, in AMNH 74313 (fig. 19A–D) a row of well-developed tubercles occurs at the same whorl height starting at the point of exposure and extending to the adoral end of the phragmocone. They are less prominent than the ventrolateral tubercles and occur on every rib at approximately equal distances of 2–3 mm.

The suture in microconchs is similar to that in macroconchs (fig. 17).

JAWS: AMNH locality 3194, Weston County, Wyoming, yields an abundance of lower jaws (fig. 21). The jaws appear as isolated occurrences and are attributed to *Hoploscaphites sargklofak*, n. sp. The lower jaw is characteristic of the Aptychophora and consists of a pair of symmetrical wings separated by a slit down the middle (Landman et al., 2010).

DISCUSSION: Examination of the size difference between dimorphs in our sample of *Hoploscaphites sargklofak*, n. sp., reveals that the smallest microconch is smaller than the smallest macroconch, and that the largest microconch is smaller than the largest macroconch (fig. 8). In the sample from AMNH locality 3435, the dimorphs do not overlap in size, although the difference between the largest microconch and the smallest macroconch is only 2 mm (fig. 9). Thus, size alone is not a reliable indicator of dimorphism. However, fortunately in scaphites, other criteria such as the degree of uncoiling and ornament of the body chamber serve to distinguish dimorphs (Cobban, 1969). The implication is that a failure to recognize dimorphism on the basis of size alone in instances where no other morphological criteria are available (degree of coiling or ornament) does not necessarily imply that dimorphism does not exist, as recently pointed out by Kennedy (2003: 440) in his discussion of the Cenomanian planispiral ammonite *Schloenbachia*.

In the Western Interior, *Hoploscaphites sargklofak*, n. sp., is similar to undescribed forms of *Hoploscaphites* in the *Baculites baculus* and *B. clinolobatus* zones. It differs from the form in the underlying *B. baculus* Zone in being more compressed, with more flattened flanks, a larger

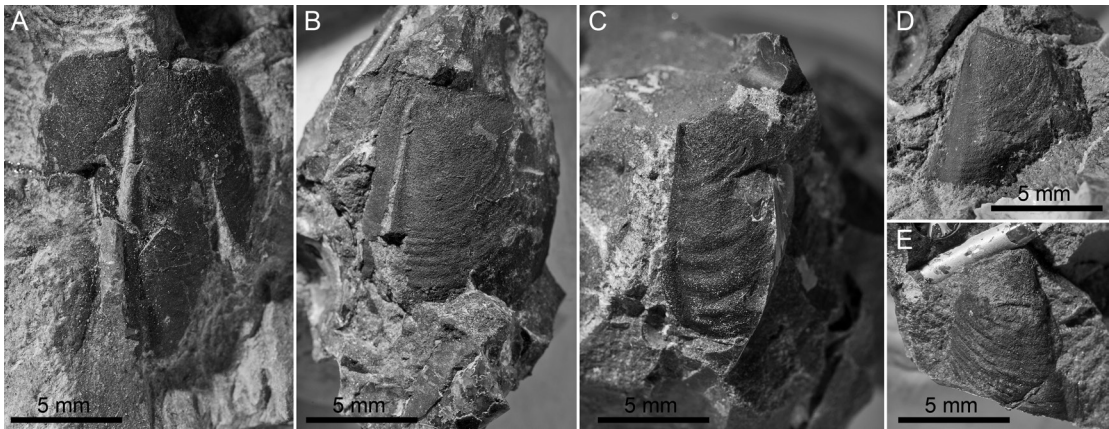


FIG. 21. Lower jaws of *Hoploscaphites sargklofak*, n. sp., AMNH loc. 3194, Weston County, Wyoming. A. AMNH 64663, lower jaw with commissure exposed. B. AMNH 64663, lower jaw, slightly rotated to expose the left side. C. AMNH 63588, lower jaw, left side. D. AMNH 64635, lower jaw, left side. E. AMNH 64649, lower jaw, right side.

umbilicus, more numerous and closely spaced ventrolateral tubercles, and, in some specimens, lateral tubercles on the adapical one-half of the phragmocone and on the hook. It differs from the form in the overlying *B. clinolobatus* Zone in being less compressed and with more rounded flanks, broader venter, and fewer ventrolateral tubercles. Thus, the biostratigraphic sequence of these three species from the *B. baculus* to the *B. clinolobatus* Zones reveals a trend in *Hoploscaphites* toward greater shell compression and smaller, more numerous ventrolateral tubercles.

Outside the Western Interior, *Hoploscaphites sargklofak*, n. sp., most closely resembles *H. constrictus* Sowerby, 1817, from northern Europe (see Kennedy, 1986: pl. 13, figs. 1–3, 16–24; pl. 14, figs. 1–38; pl. 15, figs. 1–31; text-figs. 9, 11; Machalski, 2005, figs. 5–7, 10, 12). This species ranges from the base of the Maastrichtian to the Cretaceous/Paleogene boundary and possibly into the lower Paleocene (Machalski and Heinberg, 2005). This range overlaps with that of *Hoploscaphites sargklofak*, n. sp., which occurs in the middle part of the lower Maastrichtian.

Hoploscaphites sargklofak, n. sp., differs slightly from *H. constrictus* in its shape and details of its ornamentation. These differences are apparent in a comparison of macroconchs of similar size: (1) the number of ventrolateral tubercles on the exposed phragmocone is higher in *H. sargklofak*, n. sp., than in *H. constrictus* (compare figs. 12J and 22A); (2) the venter of the shaft is flatter and the distance between ventrolateral tubercles on either side of the venter at midshaft is greater in *H. sargklofak*, n. sp., than in *H. constrictus* (compare figs. 13K and 22C); (3) one or two rows of lateral tubercles occasionally occur on the phragmocone and, more rarely, on the hook in *H. sargklofak*, n. sp., whereas they are absent in *H. constrictus* (compare figs. 14C and 22E); and (4) the umbilicus is larger in *H. sargklofak*, n. sp., than in *H. constrictus* (compare figs. 11H and 22E).

OCCURRENCE: This species occurs in the lower Maastrichtian *Baculites grandis* Zone in several formations in the U.S. Western Interior: the upper part of the Pierre Shale in Colorado, Wyoming, and South Dakota, the Lewis Shale in Wyoming, and the upper part of the Bearpaw Shale in Montana.

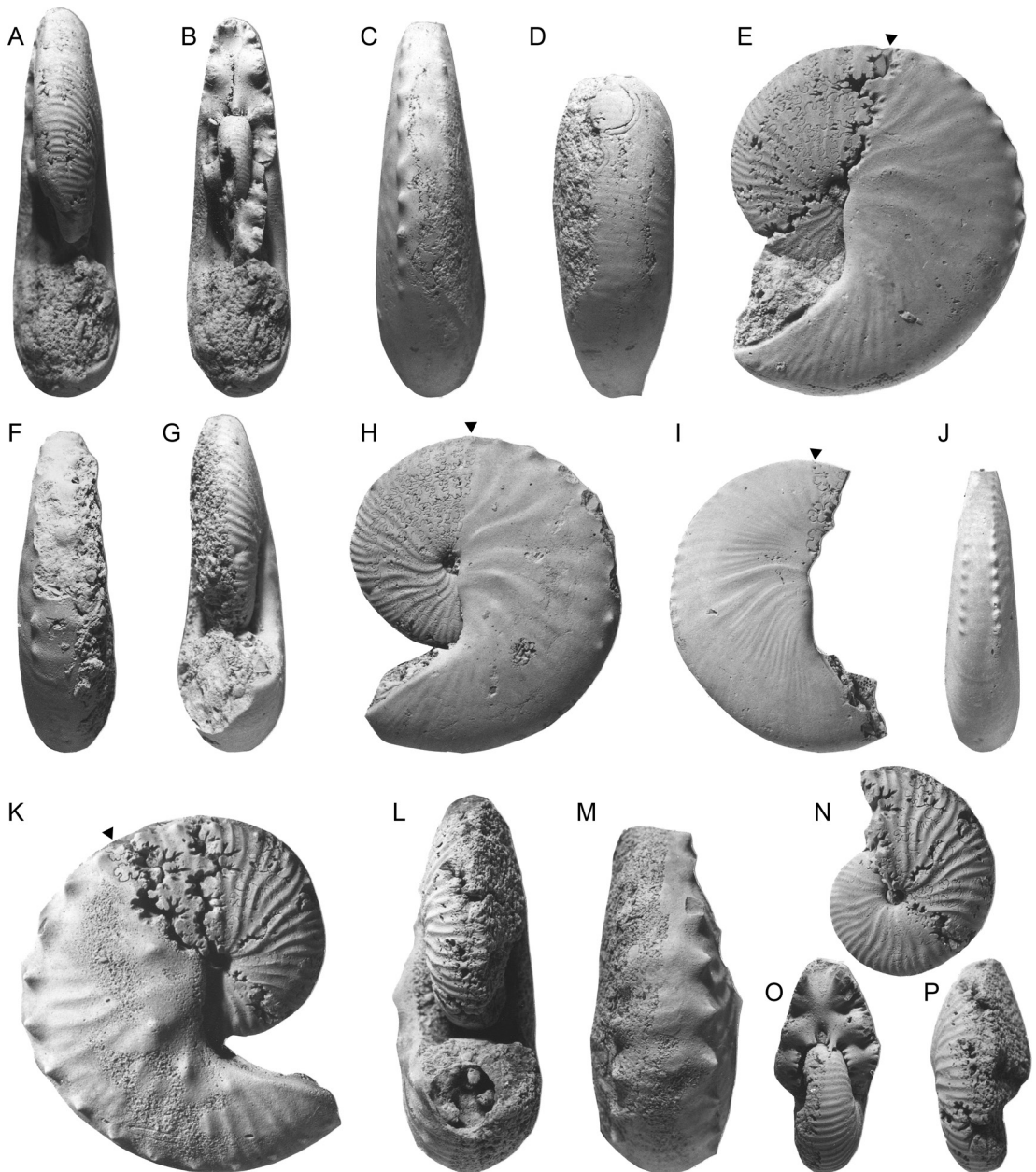


FIG. 22. *Hoploscaphites constrictus* Sowerby, 1817, macroconchs, Calcaire à *Baculites*, Cotentin Peninsula, Manche, France. A–E. SP 8, near Néhou. **A.** Apertural; **B.** apertural with part of the phragmocone removed; **C.** ventral; **D.** hook; **E.** left lateral. F–H. MNHP R1247c, “région de Ste. Colombe.” **F.** Ventral; **G.** apertural; **H.** left lateral. I, J. SP 3, Fresville. **I.** Right lateral; **J.** ventral. K–P. BMNH C43988, paralectotype, from Ste. Colombe “near Valognes.” **K.** Right lateral; **L.** apertural; **M.** ventral; **N.** right lateral, phragmocone; **O.** apertural, phragmocone; **P.** ventral, phragmocone. Specimens $\times 1$.

ACKNOWLEDGMENTS

We thank Margaret (Peg) Yacobucci (Bowling Green State University, Bowling Green, Ohio), John A. Chamberlain, Jr. (Brooklyn College, Brooklyn, New York), and Marcin Machalski (Instytut Paleobiologii, Polska Akademia Nauk, Warsaw, Poland) for reviewing an earlier draft of this manuscript and making many valuable suggestions. At the American Museum of Natural History, we thank Bushra Hussaini, Mary Conway, Kathleen Moore, and Marion Savas for accessioning material and assigning AMNH numbers, Susan Klofak for collecting fossils in the field and preparing specimens, Mary Knight for editing the manuscript for publication, and Stephen Thurston for photographing specimens and preparing figures. We thank the landowners Donley and Nancy Darnell for permission to collect on their property and Barbara A. Beasley for arranging permits to collect on the Buffalo Gap National Grassland, South Dakota. Many students and colleagues helped us collect in the field and we wish to express our thanks to Jamie Brezina, Barry and Aimee Brown, J. Kirk Cochran, Matthew P. Garb, Kimberly C. Handle, Peter Harries, Robert Jenkins, Andrzej Kaim, Isabella Kruta, Ekaterina Larina, Luke Larson, Tom Linn, Corinne Myers, Kristin Polizzotto, Remy Rovelli, Isabelle Rouget, and Kazushige Tanabe. We thank K.C. McKinney for providing help in using the U.S.G.S. collections and for retrieving locality data. This research was supported by the N.D. Newell Fund (AMNH).

REFERENCES

- Atabekian, A.A. 1979. Correlation of the Campanian stage in Kopetdag and western Europe. *In* Aspekty der Kreide Europas, International Union of Geological Sciences A6: 511–526. Stuttgart: Schweizerbart.
- Baadsgaard, H., J.F. Lerbekmo, and J.R. Wijbrans. 1993. Multimethod radiometric age for a bentonite near the top of the *Baculites reesidei* Zone of southwestern Saskatchewan (Campanian-Maastrichtian stage boundary?). *Canadian Journal of Earth Sciences* 30: 769–775.
- Birkelund, T. 1965. Ammonites from the Upper Cretaceous of West Greenland. *Meddelelser om Grønland* 179 (7): 1–192.
- Cobban, W.A. 1969. The Late Cretaceous ammonites *Scaphites leei* Reeside and *Scaphites hippocrepis* (DeKay) in the Western Interior of the United States. U.S. Geological Survey Professional Paper 619: 1–27.
- Cobban, W.A., E.A. Merewether, T.D. Fouch, and J.D. Obradovich. 1994. Some Cretaceous shorelines in the Western Interior of the United States. *In* M.V. Caputo, J.A. Peterson, and K.J. Franczyk (editors), Mesozoic systems of the Rocky Mountain region, USA: 393–413. Denver, CO: Rocky Mountain Section of Society for Sedimentary Geology.
- Cobban, W.A., I. Walaszczyk, J.D. Obradovich, and K.C. McKinney. 2006. A USGS zonal table for the Upper Cretaceous Middle Cenomanian–Maastrichtian of the Western Interior of the United States based on ammonites, inoceramids, and radiometric ages. U.S. Geological Survey Open-File Report 2006-1250: 1–46.
- Cuvier, G. 1797. *Tableau élémentaire de l'histoire naturelle des animaux*. Paris: Baudouin, xvi, 710 pp.
- Davis, R.A., N.H. Landman, J.-L. Dommergues, D. Marchand, and H. Bucher. 1996. Mature modifications and dimorphism in ammonoid cephalopods. *In* N.H. Landman, K. Tanabe, and R.A. Davis (editors), *Ammonoid paleobiology*: 463–539. New York: Plenum Press.

- Gill, J.R., and W.A. Cobban. 1966. The Red Bird section of the Upper Cretaceous Pierre Shale in Wyoming. U.S. Geological Survey Professional Paper 393-A: 1–73.
- Gill, T. 1871. Arrangement of the families of mollusks. Smithsonian Miscellaneous Collections 227: 1–49.
- Izett, G.A., W.A. Cobban, G.B. Dalrymple, and J.D. Obradovich. 1998. $^{40}\text{Ar}/^{39}\text{Ar}$ age of the Manson impact structure, Iowa, and correlative impact ejecta in the Crow Creek Member of the Pierre Shale (Upper Cretaceous), South Dakota and Nebraska. Geological Society of America Bulletin 110: 361–376.
- Kauffman, E.G., 1967. Coloradoan macroinvertebrate assemblages, central Western Interior, United States. In E.G. Kauffman and H.C. Kent (editors), Paleoenvironments of the Cretaceous seaway in the Western Interior: 67–143. Golden, CO: Colorado School of Mines Special Publication.
- Kauffman, E.G., and W.G.E. Caldwell. 1993. The Western Interior Basin in space and time. In W.G.E. Caldwell and E.G. Kauffman (editors), Evolution of the Western Interior basin. Geological Association of Canada Special Paper 39: 1–30.
- Kennedy, W.J. 2013. On variation in *Schloenbachia varians* (J. Sowerby, 1817) from the Lower Cenomanian of western Kazakhstan. Acta Geologica Polonica 63: 443–468.
- Kennedy, W.J. 1986. The ammonite fauna of the Calcaire à *Baculites* (Upper Maastrichtian) of the Cotentin Peninsula (Manche, France). Palaeontology 29: 25–83.
- Landman, N.H., and S.M. Klofak. 2012. Anatomy of a concretion: life, death, and burial in the Western Interior Seaway. Palaios 27: 672–693.
- Landman, N.H., and K.M. Waage. 1993. Scaphitid ammonites of the Upper Cretaceous (Maastrichtian) Fox Hills Formation in South Dakota and Wyoming. Bulletin of the American Museum of Natural History 215: 1–257.
- Landman, N.H., K. Tanabe, and Y. Shigeta. 1996. Ammonoid embryonic development. In N.H. Landman, K. Tanabe, and R.A. Davis (editors), Ammonoid paleobiology: 343–405. New York: Plenum Press.
- Landman, N.H., W.J. Kennedy, W.A. Cobban, and N.L. Larson. 2010. Scaphites of the “*nodosus* group” from the Upper Cretaceous (Campanian) of the Western Interior of North America. Bulletin of the American Museum of Natural History 342: 1–242.
- Landman, N.H., W.J. Kennedy, W.A. Cobban, N.L. Larson, and S.D. Jorgensen. 2013. A new species of *Hoploscaphites* (Ammonoidea: Ancyloceratina) from cold methane seeps in the Upper Cretaceous of the U.S. Western Interior. American Museum Novitates 3781: 1–39.
- Larson, N.L. In press. The cephalopod fauna from the Coon Creek Formation (Late Cretaceous) in Tennessee. Bulletin of the Alabama Museum of Natural History.
- Larson, N.L., S.D. Jorgensen, R.A. Farrar, and P.L. Larson. 1997. Ammonites and the other cephalopods of the Pierre Seaway. Tucson, AZ: Geoscience Press, 148 pp.
- Machalski, M. 2005. Late Maastrichtian and earliest Danian scaphitid ammonites from central Europe: taxonomy, evolution, and extinction. Acta Palaeontologica Polonica 50 (4): 653–696.
- Machalski, M., and C. Heinberg. 2005. Evidence for ammonite survival into the Danian (Paleogene) from the Cerithium Limestone at Stevns Klint, Denmark. Bulletin of the Geological Society of Denmark 52: 97–111.
- Nowak, J. 1911. Untersuchungen über die Cephalopoden der oberen Kreide in Polen. II Teil: die Skaphiten. Bulletin de l'Académie des Sciences de Cracovie Série B 7: 547–589.
- Riccardi, A.C. 1983. Scaphitids from the Upper Campanian–Lower Maastrichtian Bearpaw Formation of the Western Interior of Canada. Geological Survey of Canada Bulletin 354: 1–51.
- Sowerby, J. 1817. The mineral conchology of Great Britain, vol. 2. London: the author. [7 vols.]
- Wiedmann, J. 1966. Stammesgeschichte und System der posttriadischen Ammonoideen: ein Überblick. Neues Jahrbuch für Geologie und Paläontologie Abhandlungen 125: 49–79; 127: 13–81.

- Williams, G.D., and Stelck, C.R. 1975. Speculations on the Cretaceous palaeogeography of North America. In W.G.E. Caldwell (editor), *The Cretaceous system in the Western Interior of North America*. Geological Association of Canada Special Paper 13: 1–20.
- Wright, C.W. 1996. *Treatise on invertebrate paleontology: Mollusca 4, Cephalopoda: Ammonoidea*. Boulder, CO: Geological Society of America.
- Zittel, K.A. von. 1884. *Handbuch der Paläontologie*. Abteilung 1. Band 2: 329–522. Munich: R. Oldenbourg.

APPENDIX

LIST OF LOCALITIES

Localities are numbered consecutively and mapped in figure 3. Numbers 1–17 are American Museum of Natural History (AMNH) localities; numbers 18–32 are U.S. Geological Survey (USGS) localities; and numbers 33 and 34 are YPM localities. The names of collectors and dates of collection are indicated at the end of each entry, where known. In the USGS numbers, the prefix D refers to Denver locality numbers and the others refer to Washington, D.C., locality numbers.

AMNH Localities

1. 3194. Kara Bentonitic Member and upper unnamed shale member of the Pierre Shale, N¼ sec. 17, T. 46 N., R. 64 W., Osage Oilfield near Osage, Weston County, Wyoming.
2. 3264. Top of *Baculites baculus* Zone, Pierre Shale, W½ sec. 15, T. 42 N., R. 62 W., west of Newcastle, Weston County, Wyoming.
3. 3265. *Baculites baculus*–*B. grandis* zones, Pierre Shale, SE¼ sec. 15, T. 42 N., R. 62 W., west of Newcastle, Weston County, Wyoming.
4. 3269. *Baculites baculus*–*B. grandis* zones, Pierre Shale, SE¼ sec. 30, SW¼ sec. 29, NE¼ sec. 31, NW¼ sec. 32, T. 43 N., R. 62 W., west of Newcastle, Weston County, Wyoming.
5. 3278. *Baculites baculus*–*B. grandis* zones, Pierre Shale, near Newcastle, Weston County, Wyoming.
6. 3279. Top of *Baculites grandis* Zone or bottom of *B. clinolobatus* Zone, Pierre Shale, near Newcastle, Weston County, Wyoming.
7. 3435. *Baculites grandis* Zone, upper part of the Pierre Shale, 44° 14.225'N, 102° 33.173' W, Meade County, South Dakota.
8. 3487. *Baculites grandis* Zone, upper part of the Pierre Shale, 43° 35' 36" N, 104° 16' 42" W, Weston County, Wyoming.
9. 3727 (= G71188). *Baculites grandis*–*B. clinolobatus* zones, mostly in and below 8 ft bentonite noted by Gill and Cobban (1966), upper unnamed shale member, Pierre Shale, in an area trending northeast across Brewster Draw, 2.1–2.5 mi north-northeast of Redbird, from SW¼ to NW¼NE¼NE¼ sec. 14, T.38N., R.62W., Niobrara County, Wyoming, July 11, 1988.
10. 3728 (= G71288). *Baculites grandis*–*B. clinolobatus* zones, mostly in and below 8 ft bentonite noted by Gill and Cobban (1966), upper unnamed shale member, Pierre Shale, in an

area trending northeast across Brewster Draw, 2.1–2.5 mi north-northeast of Redbird, from SW $\frac{1}{4}$ to NW $\frac{1}{4}$ NE $\frac{1}{4}$ NE $\frac{1}{4}$ sec. 14, T.38N., R.62W., Niobrara County, Wyoming. July 12, 1988.

11. 3728a (= G71388). *Baculites grandis*–*B. clinolobatus* zones, mostly in and below 8 ft bentonite noted by Gill and Cobban (1966), upper unnamed shale member, Pierre Shale, in an area trending northeast across Brewster Draw, 2.1–2.5 mi north-northeast of Redbird, from SW $\frac{1}{4}$ to NW $\frac{1}{4}$ NE $\frac{1}{4}$ NE $\frac{1}{4}$ sec. 14, T.38N., R.62W., Niobrara County, Wyoming. July 13, 1988.

12. 3729 (= G71488). *Baculites grandis* Zone, mostly in and below 8 ft bentonite noted by Gill and Cobban (1966), upper unnamed shale member, Pierre Shale, in an area trending northeast across Brewster Draw, 2.1–2.5 mi north-northeast of Redbird, from SW $\frac{1}{4}$ to NW $\frac{1}{4}$ NE $\frac{1}{4}$ NE $\frac{1}{4}$ sec. 14, T.38N., R.62W., Niobrara County, Wyoming. July 14, 1988.

13. 3730 (= G71488). *Baculites baculus*–*B. grandis* zones, mostly in and below 8 ft bentonite noted by Gill and Cobban (1966), upper unnamed shale member, Pierre Shale, in an area trending northeast across Brewster Draw, 2.1–2.5 mi north-northeast of Redbird, from SW $\frac{1}{4}$ to NW $\frac{1}{4}$ NE $\frac{1}{4}$ NE $\frac{1}{4}$ sec. 14, T.38N., R.62W., Niobrara County, Wyoming. July 14, 1988.

14. 3731 (= G71588). *Baculites baculus*–*B. clinolobatus* zones, mostly in and below 8 ft bentonite noted by Gill and Cobban (1966), upper unnamed shale member, Pierre Shale, in an area trending northeast across Brewster Draw, 2.1–2.5 mi north-northeast of Redbird, from SW $\frac{1}{4}$ to NW $\frac{1}{4}$ NE $\frac{1}{4}$ NE $\frac{1}{4}$ sec. 14, T.38N., R.62W., Niobrara County, Wyoming. July 15, 1988.

15. 3732 (= G71688). *Baculites baculus*–*B. clinolobatus* zones, mostly in and below 8 ft bentonite noted by Gill and Cobban (1966), upper unnamed shale member, Pierre Shale, in an area trending northeast across Brewster Draw, 2.1–2.5 mi north-northeast of Redbird, from SW $\frac{1}{4}$ to NW $\frac{1}{4}$ NE $\frac{1}{4}$ NE $\frac{1}{4}$ sec. 14, T.38N., R.62W., Niobrara County, Wyoming. July 16, 1988.

16. 3733 (= G71788). *Didymoceras nebrascense*–*Baculites grandis* zones, Pierre Shale, in an area trending northeast across Brewster Draw, 2.1–2.5 mi. north-northeast of Redbird, from SW $\frac{1}{4}$ to NW $\frac{1}{4}$ NE $\frac{1}{4}$ NE $\frac{1}{4}$ sec. 14, T. 38N., R.62W., Niobrara County, Wyoming. July 17, 1988.

17. 3735 (= G72088). *Baculites baculus*–*Hoploscaphites birkelundae* zones, upper unnamed shale member, Pierre Shale, and overlying Fox Hills Formation, sec. 14, T. 38N., R.62W., Niobrara County, Wyoming. July 20, 1988.

USGS Localities

18. 10768. *Baculites baculus*–*B. grandis* zones, Bearpaw Shale, 50 feet below top, NE $\frac{1}{4}$ sec. 26 T. 16 N., R. 38 E., Freedom Dome about 15 $\frac{1}{2}$ mi south of Jordan, Garfield County, Montana.

19. 21584. Mobridge Shale, about 112 ft above base, about 5 mi southeast of Wasta on Sage Creek Road, Haakon County, South Dakota. J.B. Reeside and W.A. Cobban, 1949.

20. 22114. *Baculites grandis* Zone at top of Pierre Shale, SE $\frac{1}{4}$ sec. 22, T. 38 N., R. 62 W., about 1 mi north of RedBird Store, Niobrara County, Wyoming.

21. 23625. ?*Baculites grandis* Zone, Bearpaw Shale, approximately 40 feet below Bearpaw-Colgate contact, upper zone of calcareous concretions, near corner between sec. 23 and sec. 26, T. 27 N., R. 52 E., Richland County, Montana.

22. 23628. Bearpaw Shale, SW $\frac{1}{4}$ SW $\frac{1}{4}$ sec. 6, T. 27 N., R. 52 E., Roosevelt County, Montana.

23. 24312. Bearpaw Shale, 38 feet below top, 5 mi south-southwest of Poplar, on west side of Redwater Creek Valley, E $\frac{1}{2}$ NW $\frac{1}{4}$ sec. 2 T. 26 N., R. 50 E., McCone County, Montana. W.A. Cobban, 1951.

24. D396. *Baculites grandis* Zone, Pierre Shale, from gray limestone concretions near top of upper member, 3 mi east-northeast of Moorcroft, SE $\frac{1}{4}$ sec. 27 T. 50N., R. 67W., Crook County, Wyoming. W.J. Mapel, July 19, 1955.

25. D1033. *Baculites grandis* Zone, Pierre Shale, from brown and gray calcareous concretions 364–394 feet below top, about 1 mi southeast of U. S. Highway 85 in NW $\frac{1}{4}$ sec. 25, T. 39 N., R. 62 W., Niobrara County, Wyoming. W.A. Cobban, September 29, 1956.

26. D1275. *Baculites grandis* Zone, Bearpaw shale, 112 feet below top, E $\frac{1}{2}$ NE $\frac{1}{4}$ sec. 34, T. 16 N., R. 37 E., Garfield County, Montana.

27. D1986. Upper part of *Baculites grandis* Zone, upper unnamed shale member, Pierre Shale, NW $\frac{1}{4}$ SE $\frac{1}{4}$ sec. 14, T. 38 N., R. 62 W., Niobrara County, Wyoming.

28. D2118. Lower part of *Baculites grandis* Zone, upper unnamed shale member, Pierre Shale, brown limestone concretions, NW $\frac{1}{4}$ SE $\frac{1}{4}$ sec. 14, T. 38 N., R. 62 W., Niobrara County, Wyoming.

29. D2775. *Baculites grandis* Zone, Pierre Shale, NW $\frac{1}{4}$ SW $\frac{1}{4}$ sec. 32, T. 1 N., R. 70 W., Boulder County, Colorado.

30. D3194. Bearpaw Shale, 50–100 feet below top, 2000 ft north of SW corner sec. 25, T. 16 N., R. 38 E., 500 ft southwest of GP-NP 5-25-P well, Jordan Coal Field, Garfield County, Montana.

31. D6381. *Baculites grandis* Zone, Lewis Shale, NW $\frac{1}{4}$ NW $\frac{1}{4}$ NW $\frac{1}{4}$ sec. 25 T.14N, R. 90W, Carbon County, Wyoming. J.R. Gill, August 27, 1967.

32. D11783. Upper part, Pierre Shale, SE $\frac{1}{4}$ NW $\frac{1}{4}$ sec. 17, T.46 N., R.64 W., Weston County, Wyoming.

YPM Localities

33. A4768. Lower part of *Baculites grandis* Zone, in and below 8 ft bentonite noted by Gill and Cobban (1966), upper unnamed shale member, Pierre Shale, in an area trending northeast across Brewster Draw, 2.1–2.5 mi north-northeast of Redbird, from SW $\frac{1}{4}$ to NW $\frac{1}{4}$ NE $\frac{1}{4}$ NE $\frac{1}{4}$ sec. 14, T.38N., R.62W., Niobrara County, Wyoming.

34. A4778. ?*Baculites baculus* Zone, upper unnamed member, Pierre Shale, unit 89 of Traverse A (Gill and Cobban, 1966), gully west of fence, NW $\frac{1}{4}$ NW $\frac{1}{4}$ NE $\frac{1}{4}$ NW $\frac{1}{4}$ sec. 23, T. 62 N., R. 38 W., 1.8 mi northeast of Redbird, Niobrara County, Wyoming.